Astron. Astrophys. 272, 77–97 (1993)

ASTRONOMY AND ASTROPHYSICS

New globular cluster candidates in the inner regions of M 31 and the projected density profile of the cluster system

P.L. Battistini[1], F. Bònoli[1], M. Casavecchia[1], L. Ciotti[13], L. Federici[2], and F. Fusi Pecci[12]

[1] Dipartimento di Astronomia, Università di Bologna, CP 596, I-40100 Bologna, Italy
[2] Osservatorio Astronomico, Via Zamboni 33, I-40126 Bologna, Italy
[3] Present address: Princeton University Observatory, Peyton Hall, 08544 NJ, USA

Received December 13, 1991; accepted October 20, 1992

Abstract. A new search for globular clusters carried out in the inner regions of M 31 (within about 1 kpc from the nucleus, ~ 5.5 arcmin) has yielded 3 Bo-class A, 1 B, 20 C, and 20 D new candidates never included in any previous list (see Battistini et al. 1987), and has allowed us to revise the classification of all those already detected in the same area.

The total sample of possible candidates ever proposed so far has then been carefully revised, leading to the definition of the "current best sample" of M 31 cluster candidates including 341 objects.

By considering the numbers of globular clusters detected in M 31 and in the Galaxy over annuli at increasing galactocentric distances, a total population ratio of about 2.5 ± 1.0 (conservative error) has been adopted, and the total number of M 31 clusters outside a radius of ~20 kpc should be ~65. In particular, 15-20 new clusters should be detected in the annulus 20-30 kpc, partially scanned by the available surveys, but the task is difficult since most of them should be fainter than V=18 and Palomar-like.

A second sample, the "adopted best sample", thought to be sufficiently uncontaminated, homegeneous, and complete (up to about 25 kpc from the M 31 nucleus and down to V~ 18) and including 298 clusters, has then been defined to study the projected cluster density profile and to address the long-standing question of the so–called *missing* globulars with respect to the centrally extrapolated $R^{1/4}$–law.

The analysis of the spatial distribution has shown that:

i) Adopting a $R^{1/4}$–law, the *fitted effective* radius of the system, $R_{\rm ef}$, is highly sensitive to any variation of the adopted sample but it does not differ significantly from the *observed* value, $R_{\rm eo} \sim 4.59$ kpc if a sufficiently unbiased sample is used. However, various tests show that the proposed $R^{1/4}$–law is not necessarily the best fitting description of the observations.

ii) Assuming $R_{\rm e} = R_{\rm eo}$, a best fitting procedure based on $R^{1/m}$–laws yields $m \sim 1.6$ as the optimal solution. This would imply that the *spatial* distribution of the globular clusters in the central regions of M 31 is much flatter than the behaviour typical of the $R^{1/4}$–law.

iii) Fitting the data with R^{-n}–laws turns out to be worse for any value of n, the best being n =0.9 if equal weights are assigned to all radial bins.

iv) Various tests show that the best fitting description of the observations, the quality of the fit, and the deduced parameters are significantly depending on the adopted errors and weights.

v) If the validity of the $R^{1/4}$–law is imposed outside a fixed galactocentric distance (3,2,1,kpc), a residual *central flattening* persists even after this new search.

vi) The same procedure applied to the sample of Galactic globular clusters leads to similar results suggesting, if confirmed, that the effective radius of the visible halo formed by the stellar spheroidal component of the parent galaxy is smaller than that of the globular cluster system. However, the separation of true halo globulars from other globular clusters in M 31 is problematic and this may still affect the results.

Key words: galaxies: individual – galaxies: M 31 – clusters: globular – survey

1. Introduction

The importance and impact of the study of the globular cluster system in M 31 increase steeply with increasing reliability and completeness of the survey of the candidates over the full distance range going from the very central regions of the galaxy out to its far halo [100 kpc ~ 9 deg at the M 31 distance, i.e. a distance modulus $(m\text{-}M)_0 \simeq 24.07$ (de Vaucouleurs 1978)].

A complete reference to all lists of candidates since the early study carried out by Hubble (1932) can be found in Battistini et al. (hereafter *Bo–Group*) (1987,1993, in preparation) and

Send offprint requests to: L. Federici

© European Southern Observatory • Provided by the NASA Astrophysics Data System

Racine (1991). Although repeated and careful efforts have added more and more candidates and, at the same time, improved the decontamination of the catalog from spurious objects, it seems fair to say that a *complete* sample has not been achieved yet. As already stressed by Fusi Pecci (1988), the main reason for this difficulty lies in the similarity of the methods adopted for most of the searches, essentially based on visual inspection of images to distinguish cluster candidates from stars or other non–stellar objects. Three new studies (Reed et al. 1992; Aurière et al. 1992; Racine & Harris 1992) have specifically addressed the problem of identifying confirmed (mostly faint) M 31 clusters, specially by a direct scrutiny of the whole Bologna catalog of candidates (i.e. including also the C and D classes, *Bo-Group* 1987) which still represents the best available tool for this purpose.

Globular clusters in M 31 have intrinsic sizes (10 pc $\sim$ 3.3 arcsec) which make easy contamination of the candidate list by many kinds of unresolved objects, and *only deep, high angular resolution images capable of showing individual cluster stars can obviously distinguish M 31 globulars from unresolved galaxies or stars* (Racine 1991). Nevertheless, since it is very hard to cover such a wide area of the sky with deep images taken with exceptional seeing ($\sim$0.45 arcsec, FWHM, Racine & Harris 1991), a tireless survey carried out even in slightly worse observing conditions may yield useful candidates whose actual nature can then be checked with *specific* tests, thus saving a huge amount of prime telescope time.

The present Note reports on the latest step of our long–term project started in 1976 (*Bo–Group* 1980,1987) devoted to detect globular cluster candidates in M 31. In the present study we have focused our attention on the inner regions of the galaxy (within about 1 kpc from the nucleus, $\sim$5.5 arcmin) with the aim of verifying whether the *flattening* of the projected density profile for the cluster system first detected by de Vaucouleurs & Buta (1978, hereafter dVB) and later questioned by Wirth et al. (1985, hereafter WSB) is real or due to an observational effect.

Harris & Racine (1979) note that to eliminate any flattening for galactocentric distances R <3 kpc with respect to the $R^{1/4}$–law fitted by dVB to the Sargent et al. (1977) data, *some 140 objects, including 20 brighter than V=16, would have been missed in the extensively searched inner 30 arcmin diameter area of M 31*. The subsequent survey (*Bo–Group* 1987) increased slightly the number of candidates in the central region, but the flattening remained. However, *Bo–Group* pointed out that there is no doubt that very compact clusters have been lost in all the morphological surveys due to the difficulty to detect *stellar* images on the very strong and variable background made up by the body of M 31 itself.

To overcome these difficulties, WSB used a completely different approach based on the *excess–count* method. In essence, they found a statistically significant excess of bright images in the luminosity range of globular clusters in M 31 by comparing the observed luminosity distribution with the Bahcall–Soneira (1980) model of Galactic foreground stars. If identified and confirmed (their detection was in fact just *statistical*), their optical candidates would double the number of clusters in the surveyed region.

Fusi Pecci (1988) stressed the uncertainties in the procedure adopted by WSB due to fluctuations in the counts and in the model and the possible contamination of the sample by the brightest resolved objects in M 31. Moreover, he noticed a strong difference between the histogram in magnitude of the *excess–images* of WSB and that of the very compact clusters close to the Galactic center. Hence, though the validity of the result presented by WSB could not be excluded, there remained the suspicion that the discussed flattening could not be due totally to incompleteness in the available samples of identified clusters.

In order to gain further insight into this problem which has an important impact on the study of both cluster formation and survival and galactic bulges, we have used a set of CCD–frames and two large–scale plates obtained in good seeing conditions 1) to detect and measure magnitudes (BVRI) and colors of all the objects (down to V $\sim$ 19.0) in a central area of M 31, and 2) to inspect the morphology of all the images. Doing this we have obtained a small list of new candidates (at different degree of confidence) whose actual nature could then be checked by using very high resolution imaging and spectroscopy.

Section 2 describes the observational material and the reduction techniques. The catalog of the detected objects is presented in Sect. 3, including also identifications with other lists. In Sect. 4, the number and color distribution of Galactic foreground stars are estimated to confirm the existence of an excess of images possibly constituted by globular clusters. The current status of the search for globular clusters in M 31 is then schematically reviewed in Sect. 5 as far as contamination, completeness and homegeneity of the available sample of candidates are concerned. This leads to the determination of the "current best sample" of M 31 clusters which is presented in Sect. 6. Section 7 is devoted to estimate the number and detectability of the still unknown clusters in M 31 based also on a comparison with the globular cluster population in the Milky Way. Section 8 presents a sample of M 31 clusters believed to be sufficiently uncontaminated, homogeneous and complete up to about 25 kpc from the M 31 nucleus and down to V $\sim$ 18, the "adopted best sample". The detailed study of the observed projected number density profile of the globular cluster system and of its analytical representation is the subject of Sect. 9 where various alternative fitting laws are examined, and the problem of the so-called *flattening* with respect to the $R^{1/4}$–law is discussed. Finally, in Sect. 10, the comparison with the corresponding results obtained for the cluster system of the Milky Way is briefly reported.

2. Observations and reductions

In order to carry out the present search, we have used two different sets of observational material. First, we have obtained 20 BVRI CCD–frames at the 152–cm f/8 Ritchey–Chrètien telescope in Loiano (Bologna) using a SID 501 RCA chip (17 arcsec/mm, 320x512 pixels). The survey consists of 5 adjacent fields which cover a quite irregular area (see Fig. 1). The worsening of the seeing conditions during the run prevented the completion of the planned coverage. Second, we used two plates taken

© European Southern Observatory • Provided by the NASA Astrophysics Data System

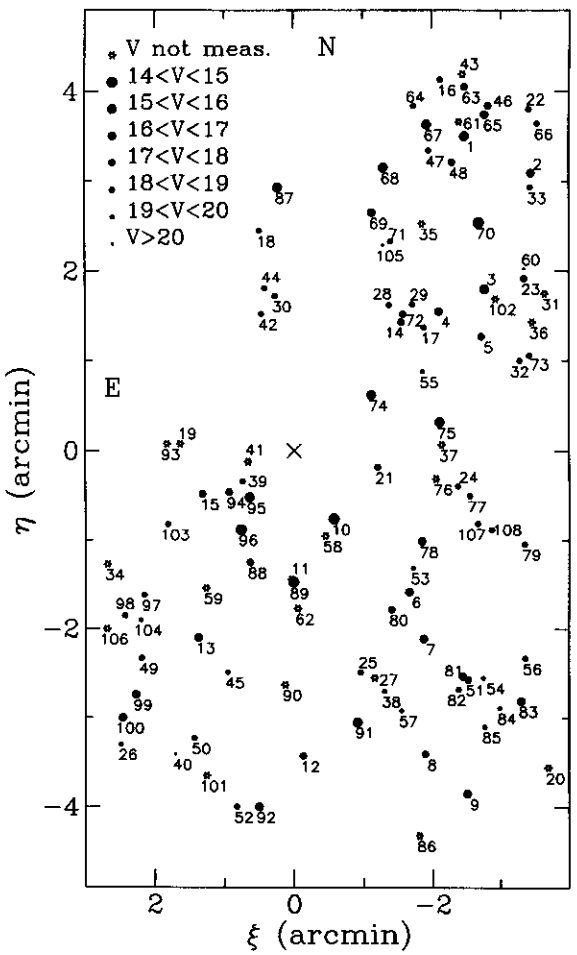

Fig. 1. Map of the observed fields. The cross indicates the position of the M 31 nucleus. The ξ, η reference system defined by Baade & Arp (1964) is used

at the f/8 Ritchey–Chrétien focus of the 4m KPNO telescope (see Table 1) by W. E. Schoening and kindly made available to us. Given their very favourable scale (~6.62 arcsec/mm) and good seeing conditions, they proved to be excellent for inspecting the image morphology of the candidates detected on the CCD–frames. A complete log of the observations is presented in Table 1.

The data reduction has been carried out using the routines included in MIDAS implemented on a VAX 8530. The searching phase was based on INVENTORY, adopting various different procedures to take into account the strong background variations across the body of M 31. Two independent searches have been done: the first, on the CCD–frames after just flat–fielding and cosmic–ray recovering, and the second, on new frames obtained by subtracting from the original ones the contribution of the main body of M 31 fitted with appropriate algorithms. The background in each frame has been estimated in 60 sub–areas and fitted with a third order polynomial. Moreover, since overlapping areas were available, cross–check identifications have allowed us to carry out tests for completeness and dependence of detection threshold on the quality of each individual frame. Finally, to minimize the level of incompleteness and to reject clearly erroneous identifications, the whole area has been inspected using a zoom to examine any possible object present in the field above a 3σ level over the local sky–noise. In this respect, it may be interesting to notice that steep background variations due to local holes or peaks in the underlying M 31 body have been sometimes detected as objects by the automatic searching routines, and only a careful visual inspection on different frames and plates can yield a sufficiently uncontaminated list of real objects.

As a result of the whole procedure mentioned above, a list of 108 objects has been obtained over the area considered (see Fig. 1) whose degree of completeness has been further tested using the procedure based on artificial stars included in DAOPHOT and available in its current version within MIDAS (July 1987). In particular, in order to determine the structural parameters of a typical template necessary to DAOPHOT to create artificial images, we have selected a set of about 10 objects on each individual frame used for the searching phase; after randomly distributing 100 artificial images on the original array, we have re–reduced the frame (starting from the search) and evaluated the fraction of known objects recovered with varying magnitude, color, and local background. The degree of completeness turned

Table 1. Observational materials.

Field#	R.A. (1950) DEC.	Date	Filters	Exps. (m)	FWHM (arcsec)
1	0 39 45 +41 01 31	1989, Oct 25	B,V,R,I	9,5,5,4	1.3
2	0 41 55 +41 10 02		B,V,R,I	9,5,3,3	1.3
3	0 42 05 +41 14 15	1989, Oct 27	B,V,R,I	9,4,3,3	1.4
4	0 42 05 +41 10 16		B,V,R,I	9,4,3,3	1.4
6	0 42 16 +41 10 23		B,V,R,I	9,4,3,3	1.4

Plate#	R.A. (1950) DEC.	Date	Emulsion, Filter	Expos. (m)	FWHM (arcsec)
139	0 41 19 +41 08 36	1974, Jul 22	IIIaJ, No filter	25	<1.0*
212	0 39 59 +41 00 03	1974, Nov 05	IIaO, GG 385	55	~1.0*

* extimated by eye, not measured yet.

© European Southern Observatory • Provided by the NASA Astrophysics Data System

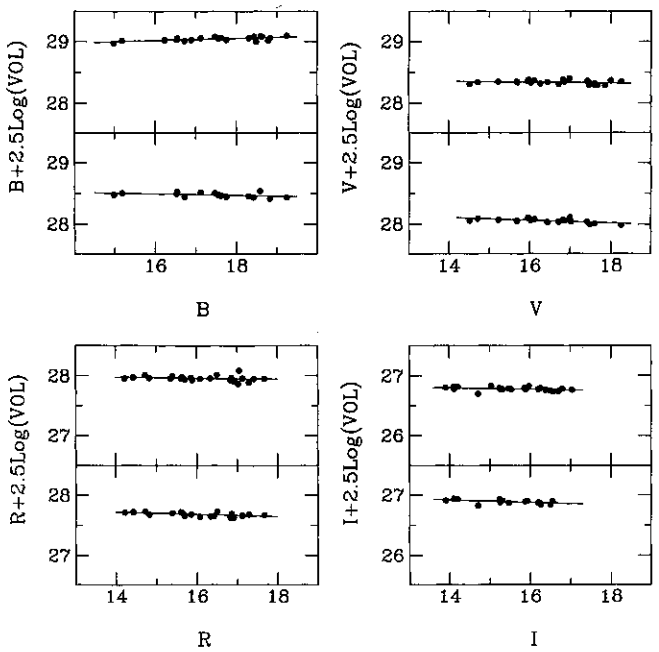

Fig. 2. Calibration curves

out to be always very close to 100% down to V∼19.0, except in the very central regions (within R <30 arcsec from the nucleus) which have been discarded as the background variations are so strong and steep that reliable detections are impossible using the available material.

Once the objects have been detected, instrumental magnitudes in each photometric band have been obtained (with MIDAS) integrating the pixel counts over a suitable area around each object, taking also in account the local background; furthermore, the exact position and a structural parameter, like the $W_{1/4}$ defined by Buonanno et al. (1982) as the half–width of the fitting surface at one fourth of its height, have been obtained for each object fitting a gaussian function to the object data. Calibration to the standard system has been made using for reference a set of stars observed in the same nights with the same instrumental apparatus in the Galactic open cluster NGC 7790 (Romeo et al. 1989). Figure 2 reports the calibration curves so obtained. All the calibrations have rms–errors less than 0.05 mag.

3. The catalog of detected objects and new candidates

Table 2 presents the final catalog including the data for all the objects detected here. As can be seen, some objects do not have the whole set of parameters, mostly because they fall at the borders of the various fields.

Column 1 gives the serial number within the present catalog. The coordinates (epoch 1950.0) given in *Columns 2,3* have been measured adopting as reference grid all the *Bo–Group* (1987) objects (at least 4–5 in each frame) present in the analysed area, the relative errors are (except for *Bo 124* and *Bo 127*) less than 1.0 arcsec.

The V–magnitude and B–V, V–R, V–I colors are listed in *Columns 4,5,6,7*. Given the already mentioned problems with the variable background, the photometric errors differ from object to object. We estimate that the errors in magnitude and color should not exceed in general 0.1–0.2 mag. This estimate stems essentially from the comparisons made with the magnitudes and colors available for the objects in common with previous studies on the same fields. In particular, the *a posteriori* identification of all the cluster candidates listed in previous catalogs has allowed a detailed comparison with previous photometries, all showing an rms less than 0.1 mag (except the comparison with the WSB data).

Column 8 gives the values obtained for $W_{1/4}$ (Buonanno et al. 1982). Since we have not used here Moffat's (1969) profiles to fit the images, the actual definition of this parameter is here slightly different, being $W_{1/4}$ =1.67σ of the Gaussian which best fits each image. We stress that we have not used this parameter to make the candidate selection and classification as they have been carried out by visual inspection on the large scale plates. We have measured $W_{1/4}$ "a posteriori". The values so obtained are seeing-dependent, and the figures listed refer to the best available CCD frame in each field. Since their quality was quite homogeneous (see Table 1), their relative comparisons are thus meaningful.

The degree of confidence in the morphological classification as globular cluster candidate made by visual inspection of the two KPNO plates is given in *Column 9*. The meaning of the different classes is the same as the one defined in *Bo–Group* (1980). In particular, the probability that the object is a cluster decreases from class A (very high) to class D (very low). Within this scheme, class E refers to objects which are not clusters or whose classification was impossible.

Finally, *Column 10* contains remarks concerning problems with measures and identifications with other catalogs.

The catalog of the 108 objects detected in the survey has been cross–checked with the data–base of the 34 catalogs of miscellaneous sources identified at different wavelengths in the M 31 area (Battistini & Guarnieri 1985). Only 51 objects have no alternative identification.

The most important conclusions one can draw from these identifications are:

i) all the globular cluster candidates present in the surveyed area and listed in any previous study have been detected;

ii) the number of objects identified with sources different from cluster candidates is very small. In particular, one has: 3 Planetary Nebulae, 1 Radio source, 13 X–ray sources;

iii) some objects can have multiple identifications depending on the adopted box. In fact, the radius of the tolerance–box is actually crucial in this procedure (the figures adopted in any cross–check are reported in parentheses in Table 2, col. 10). Due to the globular clusters' angular dimensions, the width of the box for the cross–check was chosen of 10–15 arcsec, except for the cases of comparison with catalogs in which the uncertainties on the coordinates are high;

iv) in the regions in common, a wide overlap is present with the catalog of objects published by WSB, and the comparison

© European Southern Observatory • Provided by the NASA Astrophysics Data System

Table 2. The catalog.

NB	R.A. (1950)	DEC.	V	B−V	V−R	V−I	$W_{1/4}$ (arcsec)	Class	Identifications and/or remarks
1	0 39 47.1	41 03 13	15.79	1.20	0.25	1.20	1.24	A	Bo 107(5), G 169(5), V 80(5), CRX 37(15)
2	0 39 42.0	41 02 48	16.54	1.47	0.36	1.49	1.26	A	Bo 96(5), G 158(5), V 78(5), CRX 29(15)
3	0 39 45.6	41 01 31	15.20	1.25	0.26	1.29	1.23	A	Bo 103(5), G 165(5), V 75
4	0 39 49.1	41 01 16	16.33	1.42	0.27	1.37	1.19	A	Bo 112(5), G 174(5), V 77(5), WSB1 W-2(5)
5	0 39 45.8	41 00 59	17.40	1.06	0.15	0.95	1.18	A	Bo 104(5), near FJ 88(6), compact
6	0 39 51.4	40 58 08	16.38	1.09	0.10	0.92	1.24	A	Bo 118(5)
7	0 39 50.3	40 57 36	16.05	1.27	0.22	1.21	1.25	A	Bo 115(5), G 177(5), S, V 67(5)
8	0 39 50.2	40 56 18	17.13	0.98	0.10	0.95	1.20	A	Bo 114(5), G 175(5), WSB2 S8-3(5)
9	0 39 46.9	40 55 52	16.14	1.19	0.17	1.07	1.30	A	Bo 106(5), WSB2 S8-14(5)
10	0 39 57.2	40 58 57	14.71	1.16	0.23	0.84	1.28	A	Bo 124(5), APB B3(*), J, CRX 51(15), CRX2 53(15)
11	0 40 00.3	40 58 15	14.47	1.10	0.25	0.85	1.60	A	Bo 127(5), APB B4(*), S, G 185(5)
12	0 39 59.6	40 56 17	17.09	0.99	0.15	0.56	1.29	A	Bo 126(5), G 184(5), V 66(5), WSB2 S9-9(5)
13	0 40 07.5	40 57 37	16.52	1.07	0.19	0.73	1.29	A	Bo 134(5), G 190(5), V-71(5)
14	0 39 52.0	41 01 09	17.27	1.47	0.16	1.44	1.26	B	Bo 119(5), WSB1 W-6(5), diffuse
15	0 40 07.2	40 59 14	17.78	1.26	0.43	1.29	1.15	B	Bo 132(5), WSB1 C-19(5), COLHRI 19,20(15)
16	0 39 49.0	41 03 51	18.17	1.33	0.51	1.55	1.20	A	
17	0 39 50.3	41 01 05	18.26	1.09	0.08	1.30	1.27	A	WSB1 W-4(5)
18	0 40 02.9	41 02 10	18.43	1.14	0.16	0.27	1.28	A	
19	0 40 08.9	40 59 48					1.41	A	Bo 264 C(5), near frame edge
20	0 39 40.7	40 56 09					1.07	A	Bo D53(5)
21	0 39 53.8	40 59 32	17.69	0.86	0.28	0.67	1.29	B	WSB1 W-7(5), CRX2 46(15), COLHRI 5,14,15(15)
22	0 39 42.2	41 03 31	18.41	1.52	0.44	1.71	1.02	C	
23	0 39 42.5	41 01 38	18.00	1.52	0.37	1.51	1.62	C	36W 188(15)
24	0 39 47.6	40 59 19	18.94	1.39	0.11	0.64	1.17	C	Stellar
25	0 39 55.2	40 57 14	18.21	1.71	0.74	2.06	1.07	C	
26	0 40 13.4	40 56 25	> 19				0.99	C	Cluster slightly elongated
27	0 39 54.1	40 57 10	> 19				1.17	C	
28	0 39 53.0	41 01 20	18.79	0.95	-0.10	0.99	1.02	C	
29	0 39 51.2	41 01 21	18.43	1.48	0.33	1.42	1.77	C	
30	0 40 01.7	41 01 26	18.81	1.11	-0.07	0.89	1.14	C	Stellar
31	0 39 41.0	41 01 28	> 19				0.98	C	WSB2 S6-4(5), stellar
32	0 39 42.9	41 00 43	18.82	1.02	0.16	0.93	1.04	C	WSB2 S6-1(5), stellar
33	0 39 42.1	41 02 39	18.31	1.24	0.09	0.90	0.92	C	Bo D54(5), stellar
34	0 40 14.4	40 58 27	> 19				1.62	C	HII region
35	0 39 50.4	41 02 14	> 19				1.28	C	
36	0 39 41.9	41 01 09	> 19				1.43	C	
37	0 39 48.9	40 59 47	> 19				1.57	C	
38	0 39 53.4	40 57 01	> 19				1.00	C	cluster
39	0 40 04.2	40 59 23	18.04	0.48	0.33		1.22	C	WSB1 C-11(5), CRX2 72(15), stellar
40	0 40 09.3	40 56 19	> 19				1.22	C	WSB2 S6-17(5)
41	0 40 03.7	40 59 36	> 19				1.46	C	WSB1 C-9(5) stellar
42	0 40 02.8	41 01 14	18.49	0.89	0.22	0.72	1.01	C	
43	0 39 47.2	41 03 54					1.07	D	Near frame edge, not stellar
44	0 40 02.5	41 01 31	18.47	1.95	0.54	2.24	1.36	D	Not stellar
45	0 40 05.3	40 57 13	> 19				1.03	D	Star
46	0 39 45.3	41 03 33	17.50	1.57	0.56	1.83	0.99	D	Not stellar
47	0 39 49.8	41 03 03	18.75	0.47	-0.21	0.50	0.91	D	Not stellar
48	0 39 48.1	41 02 56	17.80	1.01	0.13	0.95	0.97	D	Not stellar
49	0 40 11.9	40 57 23	18.80	1.05	0.07	0.57	0.97	D	Star
50	0 40 07.8	40 56 29	19.00	1.62	0.46	1.48	0.87	D	Slightly diffuse
51	0 39 46.9	40 57 08	17.91	1.37	0.31	1.24	1.13	D	WSB2 S8-6(5), stellar
52	0 40 04.6	40 55 43					0.90	D	WSB2 S9-2(5), near frame edge, stellar
53	0 39 51.1	40 58 24	> 19				1.16	D	
54	0 39 45.7	40 57 10	> 19				1.04	D	
55	0 39 50.3	41 00 35	> 19				0.88	D	COLHRI 10(15)
56	0 39 42.5	40 57 23					1.04	D	WSB2 S7-3(5), near frame edge
57	0 39 52.0	40 56 48	> 19				0.83	D	Extra faint open cluster
58	0 39 57.9	40 58 46	> 19				1.23	D	CRX2 62(15)
59	0 40 06.9	40 58 10	> 19				0.88	D	
60	0 39 42.5	41 01 45	> 19				1.05	D	36W 188(15)
61	0 39 47.5	41 03 22	> 19				0.92	D	CRX 37(15), not stellar
62	0 40 00.0	40 57 57	> 19				0.99	D	Not stellar
63	0 39 47.1	41 03 46	17.26	0.94	0.04	0.80	1.00	E	
64	0 39 51.0	41 03 33	18.91	1.78	0.80	1.97	0.96	E	
65	0 39 45.5	41 03 27	16.26	1.17	0.18	1.04	0.97	E	
66	0 39 41.5	41 03 21	18.92		-0.41	-0.88	0.96	E	
67	0 39 50.0	41 03 21	15.91	0.86	0.00	0.66	0.98	E	
68	0 39 53.3	41 02 52	15.48	0.99	0.08	0.85	0.99	E	
69	0 39 54.3	41 02 22	16.83	0.74	0.31	1.29	0.96	E	Bo D65(5)
70	0 39 46.0	41 02 15	14.89	1.24	0.24	1.09	0.95	E	
71	0 39 52.8	41 02 03	18.08	1.16	0.12	0.91	0.99	E	Bo 120 star(5)
72	0 39 51.9	41 01 14	17.63	1.01	0.09	1.01	1.07	E	Bo 261 C(5), WSB1 W-5(5)
73	0 39 42.1	41 00 46					0.84	E	Near frame edge
74	0 39 54.3	41 00 20	15.55	1.00	0.59	-0.05	1.64	E	

© European Southern Observatory • Provided by the NASA Astrophysics Data System

Table 2. (continued)

NB	R.A. (1950) DEC.	V	B−V	V−R	V−I	$W_{1/4}$ (arcsec)	Class	Identifications and/or remarks
75	0 39 49.0 41 00 02	15.73	0.87	0.04	0.82	0.91	E	WSB1 W-1(5), CRX 40(15)
76	0 39 49.3 40 59 24						E	WSB1 W-3(5), saturated image
77	0 39 46.7 40 59 13	18.38	0.93	-0.14	0.46	1.22	E	
78	0 39 50.4 40 58 42	16.97	1.07	0.13	0.87	1.00	E	
79	0 39 42.5 40 58 41	18.27	0.90	0.07	0.88	1.07	E	WSB2 S5-1(5)
80	0 39 52.8 40 57 56	17.74	1.34	0.14	0.94	1.05	E	Bo D64(5)
81	0 39 47.3 40 57 11	16.14	1.00	-0.04	0.65	1.00	E	WSB2 S8-5(5)
82	0 39 47.6 40 57 02	18.57	1.51	0.11	1.08	0.99	E	WSB2 S8-4(5)
83	0 39 42.8 40 56 54	16.68	0.89	-0.03	0.66	0.99	E	WSB2 S7-2(5)
84	0 39 44.4 40 56 49	> 19				1.05	E	WSB2 S7-1(5)
85	0 39 45.6 40 56 37	> 19				0.93	E	WSB2 S8-9(5)
86	0 39 50.7 40 55 24					1.02	E	WSB2 S8-2(5), near frame edge
87	0 40 01.4 41 02 39	15.58	1.04	0.17	0.64	0.99	E	
88	0 40 03.6 40 58 28	17.10	1.25	0.09	0.62	0.97	E	Bo D74(5)
89	0 40 00.5 40 58 16	> 19				1.60	E	
90	0 40 01.0 40 57 05						E	Saturated image
91	0 39 55.5 40 56 40	15.65	0.92	0.08	0.47	1.00	E	
92	0 40 02.9 40 55 43					1.01	E	WSB2 S9-3(5), near frame edge
93	0 40 09.9 40 59 48					1.15	E	Bo D80(5), COLHRI 15,17(15), WSB1 E-2(5), CRX2 84(15), near frame edge
94	0 40 05.2 40 59 15	17.52	0.99	-0.04	0.32	1.01	E	WSB1 C-16(5)
95	0 40 03.7 40 59 12	15.32	0.81	0.01	0.32	1.02	E	WSB1 C-8(5), CRX2 72,74(15), APB B2(*), COLHRI 21,24(15)
96	0 40 04.3 40 58 50	14.57	1.15	0.22	0.72	1.03	E	Bo D75(5), APB B1(*), WSB1 C-13(5), CRX2 74(15), COLHRI 21,24(15)
97	0 40 11.6 40 58 06	18.16	1.49	0.30	1.32	1.02	E	HO2 451(9)
98	0 40 13.2 40 57 52	18.42	1.19	0.21	1.00	0.95	E	
99	0 40 12.3 40 56 59	16.93	1.33	0.33	0.97	0.96	E	
100	0 40 13.3 40 56 43	16.93	1.00	0.17	0.53	0.99	E	
101	0 40 06.9 40 56 04						E	WSB2 S10-8(5), saturated image
102	0 39 44.7 41 01 24	> 19				1.02	E	
103	0 40 09.8 40 58 54	18.74	0.77	-0.02		1.00	E	WSB1 E-1(5)
104	0 40 11.9 40 57 49	> 19				1.02	E	
105	0 39 53.4 41 02 00	> 19				0.89	E	
106	0 40 14.5 40 57 43	> 19				1.00	E	
107	0 39 46.0 40 58 54	18.65	0.68	-0.20	-0.08	1.01	E	FJ 96(5)
108	0 39 45.0 40 58 50	18.38	1.30	0.04	1.19	1.42	E	FJ 48(5)

Notes to table 2:

The radius of the adopted identification box in arcsec is given, in parentheses, in col. 10.
(*) identification made on finding chart.

References to other lists:

APB	Alloin et al. (1976)	J	Johnson (1961)
Bo	Battistini et al. (1987)	G	Sargent et al. (1977)
COLHRI	Collura et al. (1990)	S	Sandage (1971)
CRX	Crampton et al. (1984-Tab.1)	V	Vetesnik (1962)
CRX2	Crampton et al. (1984-Tab.2)	WSB1	Wirth et al. (1985-Tab.2)
FJ	Ford and Jacoby (1978)	WSB2	Wirth et al. (1985-Tab.3)
HO2	Hodge (1979)	36W	Bystedt et al. (1984)

is worth of a brief analysis. Starting from the central area observed by WSB, 15 of the 49 objects included in their Table 3 have also been detected in our survey. Concerning the other 34, 31 are out of our field and 3 are too faint in our frames. However, in the region in common, we have detected 13 objects not included in their list. This demonstrates further the high level of completeness achieved in the present search, and can be explained by the different colors used in the search (B in WSB and V here). In the outer fields, WSB detected 148 objects down to B=21 (see their Table 2). Of them only 17 are included in our sample as the area in common is small and the limiting magnitude of our survey is much brighter.

From the global comparisons and considering the classification presented in *Column 9* of Table 2, we find that the present survey has detected a small set of new candidates never included in any previous list, and specifically: 3 class A, 1 B, 20 C, 20 D objects. They will hereafter join the sample of the already known candidates in this area originally constituted by 14 A, 2 B, 2 C, 7 D. Thanks to the excellent quality of the two KPNO plates it was possible to check further the morphology of the images of the already known candidates and improve their classification. This revision has modified the class–type for some of them leading to a re–distribution in 15 A, 2 B, 1 C, 0 D. In conclusion, the total distribution in classes for the new global sample of candidates detected in the surveyed area is: 18 A, 3 B, 21 C, 20 D.

© European Southern Observatory • Provided by the NASA Astrophysics Data System

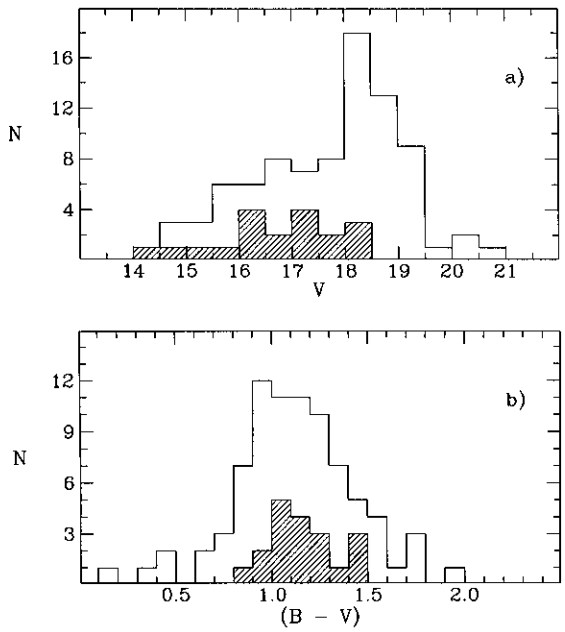

Fig. 3a,b. Histograms in V and B–V of 108 detected objects. The shaded areas show the distributions of the A and B class candidates

Figure 3 shows the histogram of the V–magnitudes and B–V colors (when available) for the 108 objects listed in Table 2. The distribution of the A+B candidates is hatched in the various figures, showing that they cover quite a wide range both in luminosity and in color. The existence of many candidates with colors (B–V $>$ 1.0), significantly redder than the mean clusters located in the outer regions (Elson & Walterbos 1988; *Bo–Group* 1993) is probably due to reddening within M 31 itself but it could also be a consequence, at least in part, of a higher metallicity.

The increasing incompleteness of the sample for V$>$19.0, much fainter than the faintest class A+B candidate, is quite evident. Due to the high reddening, most of the A+B candidates are probably intrinsically brighter and their apparent luminosity function is thus not representative of their properties. Adopting a true distance modulus of $(m\text{-}M)_0 \simeq 24.07$ the brightest cluster in the A+B sample would have, as lower limit, M_V=-9.9.

Although, as already noted above, the reliability of parameters like $W_{1/4}$ to describe, over the full intensity range, the actual image structure is somewhat seeing-dependent and decreases when the object is superimposed on a strong and variable background, Fig. 4 shows that it is still possible to distinguish the difference between candidate clusters and stellar objects using $W_{1/4}$. In fact, the histogram presented in Fig. 4 is clearly bimodal and the A+B candidates occupy the peak at larger $W_{1/4}$–values. There is of course some overlap which can however be easily understood if one notes that a very compact cluster (like M80 in the Milky Way) would appear almost indistinguishable from a normal star at the distance of M 31. This indicates that there are probably other clusters (very compact) which could escape the present selection due to the stellar nature of their images.

For completeness, we add then a few notes on the comparison of the present results with those gotten by a similar study by

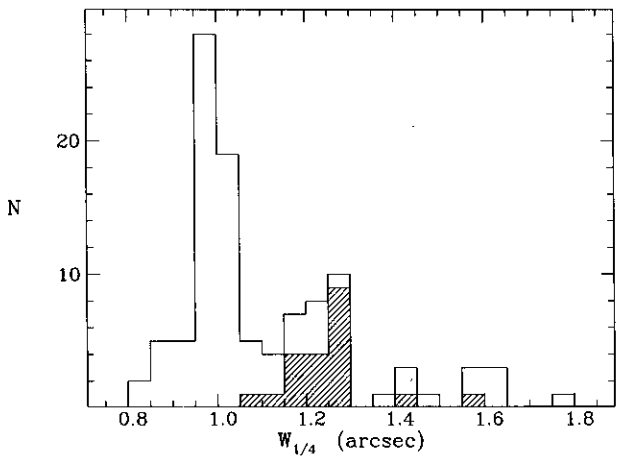

Fig. 4. Histogram of the $W_{1/4}$–values of 108 detected objects. The shaded areas show the distributions of the A and B class candidates

Table 3. Analysis of the new candidates by Aurière et al. 1992.

ACH	NB	Comments
Bo96	2	
Bo103	3	
Bo104	5	
Bo107	1	
Bo112	4	
Bo114	8	
Bo115	7	
Bo118	6	within 5" DEC.
Bo119	14	
Bo124	10	
Bo126	12	
Bo127	11	
Bo262		out field
Bo131		out field
Bo132	15	
Bo134	13	
Bo264	19	
Bo136		out field
Bo138		out field
Bo143		out field
Bo144		out field
Bo146		out field
Bo148		out field
01	20	within 6" DEC.
02	51	
03	47	
04	35	
05	21	
06	39	within 1" DEC.
07		out field
08		out field
09	45	within 4" R.A.,4" DEC.
10		out field
11		out field
12		out field
Bo261	72	
13	67	
14	17	
15	34	within 2" DEC.

Aurière et al. (1992, hereafter ACH92) and kindly made available to us by Dr. Aurière after submission of our report. ACH92 investigated a 7.7×7.7 *arcmin* field centered on the nucleus of M 31, and detected 23 globular clusters candidates already listed in the catalog of *Bo-Group* (1987). Furthermore, they discov-

© European Southern Observatory • Provided by the NASA Astrophysics Data System

ered 12 new high-confidence candidates and 4 "possible" ones. In Table 3, we present thus the identifications with the objects listed in Table 2 and some useful comments. As can be seen, all the objects ACH92 detected in the common area are also present in our search. Though the individual classifications are occasionally fairly different, there is an overall agreement in the number of clusters one could add to the previous list of Class A + B objects in the area surveyed. In fact, normalizing to the area covered by ACH92 and considering only the high confidence candidates, the list by ACH92 include 35 objects and the one presented here would lead to 34.

4. The Galactic foreground stars

A first indication on contamination of the central sample and an upper limit to the number of *possible* clusters can be obtained by comparing the luminosity and color distribution of the 108 detected objects with those predicted from the Galactic foreground models.

In order to determine the contribution of stellar images in the surveyed areas due to the Galactic foreground stars, we have adopted the Ratnatunga & Bahcall (1985) model (hereafter RB) which predicts the numbers of stellar objects in a given magnitude range with varying B-V intervals at a given Galactic latitude and longitude (b =21°.7 and l =121° adopted here for M 31). According to the Authors, the accuracy of this model is about ± 20% in the numbers and ± 0.2 mag in luminosity. Figure 5a,b,c shows the histograms of our 108 detected images (down to V=19) binned in apparent magnitude and separated into three color groups (B-V<0.8; 0.8<B-V<1.3; 1.3<B-V). Also shown

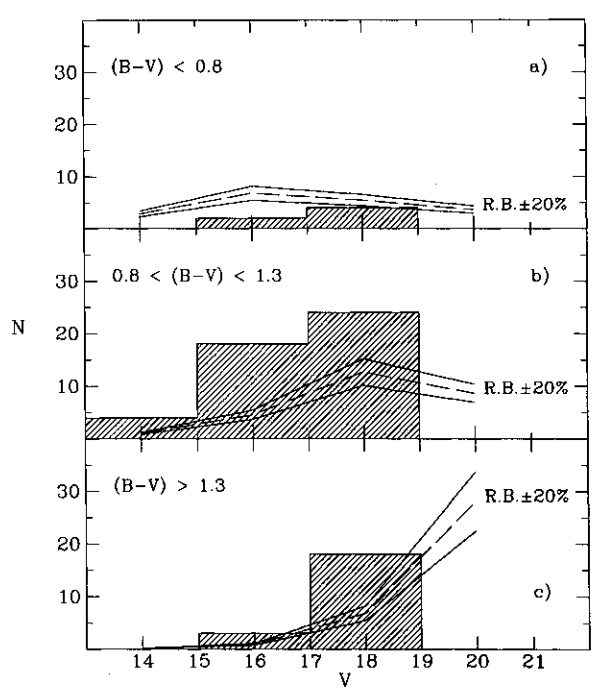

Fig. 5. Number of objects per mag per color index found in the analysed area compared with the number of stars predicted by the RB model in the same area

is the RB model (with the quoted uncertainty) normalized to our 45.3 arcmin^2 surveyed area. It appears that at intermediate colors a significant fraction of the objects detected are not due to the Galactic foreground. Similar conclusions were already reached by WSB.

Some of those objects may in fact be very bright stars members of the incipiently resolved M 31 bulge. At the limit of the present survey (V=19.0), the corresponding absolute magnitude of M 31 stars would be brighter than M_V ~-5. The predicted number of such bright objects is strongly function of the assumptions made in various star formation models for the M 31 bulge (see WSB Sect. 5 for a discussion). It would also be quite easy to construct a model which might interpret *all* excess images as due to bright M 31 stars. However, at variance with the data available to WSB, we now have some information on the image morphology and know from Fig. 4 that there is a subsample of the detected objects which appear to be *non–stellar* on large scale plates. Hence, we are inclined to exclude the hypothesis that the vast majority of the excess images (with respect to the foreground star counts) could be bright stars, thus putting on a much firmer grounds the indications on M 31 bulge stellar populations drawn by WSB.

5. M 31 globular cluster candidates: contamination, completeness, and homogeneity

A substantial effort has been done by a number of Authors to produce a complete, uncontaminated, and unbiased sample of M 31 globular clusters. The problems related to contamination, completeness and homogeneity of the search have been widely discussed for instance by Harris & Racine (1979), *Bo-Group* (1980,1987), and, recently, by Racine (1991), Reed et al. (1992), and Racine & Harris (1992). There is a general consensus that the available observational data are still quite far from satisfactory in this respect, and that the achievement of the final goal is very difficult.

Most of the recent studies (e.g. Racine 1991; Reed et al. 1992; Racine & Harris 1992) have essentially worked at getting "optimal" samples of clusters located in the outer M 31 halo to avoid reddening problems within M 31 itself and to construct a "clean" M 31 globular cluster luminosity function (GCLF). This approach is especially well suited to the purpose of using the GCLF as a useful distance indicator (Harris 1991). Distant clusters are also crucial to estimate the M 31 total mass via the cluster system kinematics (Huchra et al. 1991; Federici et al. 1990,1993). However, to study the projected number density profile as we aim at here, we must have a reliable sample all over the M 31 cluster system, including the central regions. In particular, we must:

i) Decontaminate the available sample. Since the nature of contaminating objects varies with varying galactocentric distance and also distance from the M 31 major axis, this can be done using various complementary procedures.
ii) Set some specific photometric constraints for the adopted candidates to optimize the homogeneity of the sample, thus reducing the importance of spurious selection effects.

© European Southern Observatory • Provided by the NASA Astrophysics Data System

iii) Evaluate the impact on our results and analysis of problems like internal reddening within M 31 itself, separation between disk and halo population (if any), different assumptions on the level of confidence in the reliability of the still non-confirmed candidates.

Before proceeding, it is worth examining briefly these various aspects and summarizing the present status of the survey to explain how we arrived to the definition of "the currently best sample" of M 31 clusters adopted in the following sections.

5.1. Contamination

Recent images, secured with subarcsecond seeing at the CFHT by Heasley et al. (1988), Christian & Heasley (1991), and Racine & Harris (1991,1992), clearly show resolution of the brightest stars in many M 31 globulars and provide a powerful tool for distinguishing real globular clusters from contaminating galaxies. Before these high resolution observations became possible, the confirmation of the actual nature of the candidates was feasible only via spectroscopy coupled with image analysis (Huchra et al. 1991; Federici et al. 1990,1993, and references therein). Merging the information provided by both techniques, it turns out that about half of the total candidates ever listed in the various catalogs has been checked so far, mostly in the brighter part of the GCLF.

Since these direct approaches require excellent seeing conditions, integrated color indices and image structure have also been frequently used to provide further tools to remove spurious objects from the sample (*Bo-Group* 1980,1987,1993; Elson & Walterbos 1988; Reed et al. 1992). Unfortunately, this photometric method which is quite effective for selecting clusters located in the outer M 31 halo, may become misleading in the inner regions as other factors like reddening and cluster metallicity could significantly alter the observed integrated colors.

Turning to the best available sample, the current status of the decontamination process based on the three main quoted techniques can be summarized as follows:

• *The global sample of candidates:*

By adding toghether all the objects included at least once in a list of M 31 globular cluster candidates (at any confidence level) one totalizes 1028 objects. A detailed collection of data and information about each of them is postponed to a future paper presenting a complete revised catalog and discussion of the M 31 cluster system (Battistini et al. 1993, in preparation). The reference tools in the latest studies have generally been the surveys by Sargent et al. (1977), including 355 candidates, Crampton et al. (1985), listing 509 candidates, and *Bo-Group* (1980,1987), which includes 870 objects divided into four classes with decreasing degree of confidence (254 A, 99 B, 152 C, and 334 D, plus 31 out of field). These candidates are located in a region of the sky of about $3^o \times 3^o$ centered on M 31, corresponding to $\sim 30 \times 30$ kpc at the M 31 distance. The magnitudes range covered by these objects spans from V $\sim$ 14 up to V $\sim$ 20. The actual nature of most of the objects fainter than V $\sim$ 17.5 (corresponding to $M_V \sim -6.9$) has never been checked with the best techniques, and this explains why the M 31 GCLF is still not properly known.

• *Radial velocities:*

Major lists of radial velocities of M 31 cluster candidates have been published so far by van den Bergh (1969), Huchra et al. (1991, and references therein), Peterson (1989), and Federici et al. (1990,1993). Various other groups are also known to have secured spectroscopic observations, but their data-sets are still unpublished.

Based on the published data, 181 candidates have been confirmed to be clusters on spectroscopic grounds. They have thus at least one measure of the radial velocity, and frequently have two or three independent values.

Note that two objects, *Bo 121* and *Bo 175* not included in the catalogs of *Bo–Group* and Sargent et al. (1977) because classified as *stellar*, have been included as spectroscopically confirmed by Huchra et al. (1991). Since their velocities are equal to -3 and +76 km/sec respectively, there is however in our view some doubt on their actual nature.

• *High-resolution imaging:*

As mentioned above, deep CCD high-resolution images have been obtained by various groups for a wide set of M 31 cluster candidates. Based on the published data (Racine 1991; Racine & Harris 1992; Cohen & Freeman 1991), 127 objects were observed and their intrinsic nature has been specifically checked with this technique. In total the number of confirmed clusters is 81. Of them 48 also have radial velocities. Note that at large galactocentric distances from the M 31 nucleus, almost all the contaminating objects are galaxies whose image structure is totally indistinguishable on morphological grounds from that of a normal M 31 cluster. Racine (1991) observed also 23

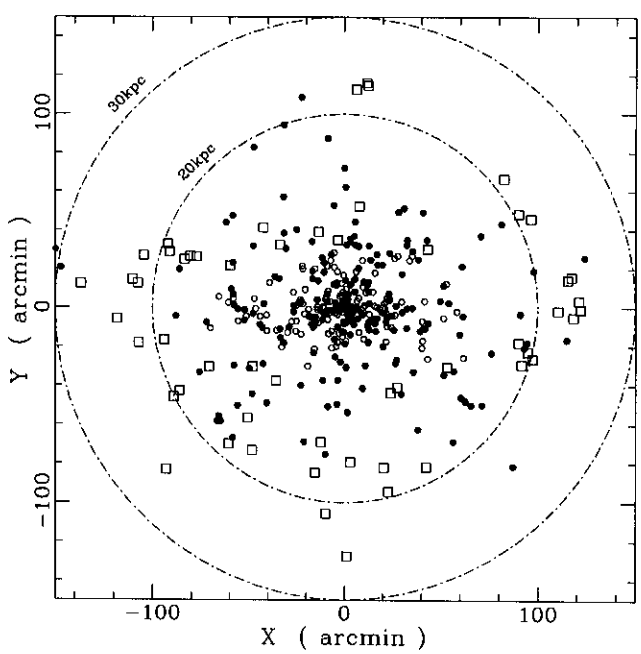

Fig. 6. Map of the projected distribution of the confirmed clusters (filled dots), high confidence cluster candidates not checked yet (open dots), and confirmed galaxies (open squares). The high incidence of galaxies among the outer candidates is apparent. The X, Y reference system defined by Baade & Arp (1964) is used

© European Southern Observatory • Provided by the NASA Astrophysics Data System

C, D class candidates taken from *Bo-Group* (1987), and found 5 clusters. The quite lower fraction of success in the C and D classes is not a surprise due to the low confidence ranking of these candidates. Concerning classes C and D, Racine & Harris (1992) have recently published the result of further observations yielding 14 confirmed clusters and 5 probable clusters over 92 observed objects.

In conclusion, taking into account the overlap between spectroscopic observations and high-resolution imaging, a total of 275 candidates have been investigated. 213 are confirmed clusters, 55 are galaxies, 6 stars, and 1 is an HII region. 181 of them have known radial velocities.

Figure 6 shows a map of the projected distribution of the confirmed clusters (filled dots), the high confidence cluster candidates not checked yet (open dots), and the confirmed galaxies (open squares).

• *Integrated color indices and image structure:*
Figure 7 shows that of the confirmed clusters and galaxies with galactocentric distance larger than 50 *arcmin*, the 31 identified galaxies have color indices in the interval $0.6 < (B-V) < 2.0$ whereas only one of the 62 confirmed clusters with measured colors has $(B-V) > 1$. Rejection of red outlying candidates seems therefore very effective in reducing the contamination from galaxies, as already suggested by *Bo-Group* and Racine (1991).

Reed et al. (1992) have made an extensive use of the color indices as classifiers by setting empirical limits to the regions of the two color diagram (B-V, V-R) occupied by confirmed clusters. To help in the classification, they have also used image growth curves.

The use of photometric procedures to select "confirmed" clusters is quite effective in the outer regions of M 31 once proper color boundaries are defined. Its application to the inner clusters, as we will necessarily do in Sect. 6.2 to define the current best sample, must be done with particular caution.

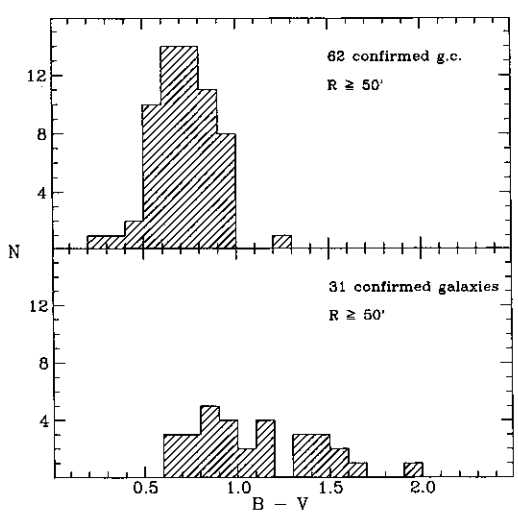

Fig. 7. Distribution of the $(B-V)$ colors of the 62 confirmed globular clusters with projected distances larger than 50 *arcmin* ($\sim$ 10kpc) from the center of M 31 and of the 31 identified galaxies

5.2. Homogeneity of the samples

The problem of the degree of homogeneity of the cluster surveys was extensively dealt with by *Bo-Group* (1987), the last, broad and independent survey carried out on M 31. It was shown there that the search phase can be considered to be sufficiently homegeneous for the candidates brighter than V $\sim$ 18. Since that catalog has been taken as reference for all the subsequent studies, one has just to briefly analyse if and how the additional candidates found later and those discarded meanwhile have modified the previous situation in this respect.

The main modifications to the "original" homogeneity come from two reasons. First, the search presented here (and the corresponding one carried out by ACH92) has led to detect in the central regions a group of candidates much fainter than the average population detected so far in the outer area. Second, thanks to the specific checks carried out in the outer halo with spectroscopy and high-resolution imaging on C and D class objects (usually fainter than those included in the A,B classes), a group of faint confirmed clusters have been detected in the outer halo which do not have a counterpart elsewhere.

These two items should be taken into account while producing the best sample to consider in the following analysis to avoid the introduction of selection bias.

5.3. Completeness

The survey carried out by *Bo-Group* (1987) was claimed to be essentially complete down to V$\sim$ 18. Since no other subsequent search has detected any significant population of candidates brighter than such a magnitude limit, it seems conceivable to assume that the vast majority of the bright (V < 18) M 31 globular clusters has been detected. Since at the distance of M 31 V $\sim$ 18 corresponds to about $M_V \sim$ -6.5, incompleteness in the sample starts becoming important soon after the expected peak of the GCLF (*Bo-Group* 1987). In their recent study, Racine & Harris (1992) have purposely investigated the nature of the faint candidates in the Bologna catalog (mostly classes C,D) to detect clusters populating the faint part of the GCLF and located in the far M 31 halo. Beyond the 2-degree ellipse defining the outermost extent of the M 31 disk, they have identified a sizeable number of clusters fainter than V $\sim$ 18. But it can hardly be stated that completeness has been achieved there for two main reasons. First, though the search of the C and D candidates was extremely careful, no claim of completeness was made by *Bo-Group* for these low-confidence, faint candidates. Second, even getting high-resolution images it is still difficult to assign a certain classification to the faintest candidates due to the paucity of giant stars which can make the resolution less obvious (Racine & Harris 1992).

A similar warning can be made about the cluster population detected in the very central regions. In fact, although the total number of candidates has been increased, reaching somewhat fainter than V $\sim$ 18, it is still possible that some very compact clusters have not been detected as their images appear "perfectly" stellar when superimposed on the strong M 31 background.

© European Southern Observatory • Provided by the NASA Astrophysics Data System

In conclusion, to be conservative, one can assume that the degree of completeness of the available surveys is high all over the M 31 cluster system down to V $\sim$ 17.5-18.0, and then decreases in a different way with varying position in the galaxy, being a bit higher in the very inner and very outer regions.

6. The "current best sample" of M 31 globular clusters

We are aware of the fact that the reliability of any study devoted to determine the $\Sigma - R$ law (see Sect. 9) for the M 31 GCS will remain low until the effects of sample incompleteness and contamination, internal reddening, and mixture of cluster populations (disk and halo) are properly known. However, if we adopt a sample properly chosen where all these effects have been minimized by the selection, we can already get some important hints on the actual behaviour, to be verified as soon as new and better data are available. It is also quite obvious that "best" is necessarily a compromise between sample size, homogeneity with respect to R and probability of membership.

To understand how we selected the samples adopted in the following, we add a few considerations on the internal reddening within M 31. In Sect. 7.2 we will later deal briefly with the discussion of the impact on our results of the distinction (if any) between "disk globulars" and those belonging to the "spheroidal" component, in analogy to what found in the Milky Way (see Zinn 1985,1986).

6.1. Internal extinction within M 31

The difficulty in determining the individual reddening of each cluster is a major problem in the study of the M 31 cluster system. Problems like determination of a safe GCLF (with varying galactocentric distance) or detection of metallicity gradients (if any) cannot achieve any firm solution until this lack of knowledge persists.

Various attempts have been made so far to face this specific problem (see Crampton et al. 1985; Iye & Richter 1985; Sharov & Lyutyi 1986, 1989; *Bo-Group* 1987; Elson & Walterbos 1988, for references). However, apart from the data obtained for a small set of the brightest clusters by L. Searle and reported by Frogel et al. (1980), the available information is quite meager.

Unfortunately, we do not have at this stage any new result on this issue. In the process of defining the "current best sample", we must thus limit ourselves to set judicious conditions on the candidates to be included in the sample.

In particular, after various tests, we have decided to separate the whole sample of M 31 cluster candidates into two sub-sets. The first, the *outer set*, includes all the candidates located outside the isophote No. 1 of de Vaucouleurs (1958) which in our view includes the bulk of the M 31 body, and the second, the *inner set*, includes the objects inside that isophote. Doing this, we have then assumed for simplicity that the clusters in the *outer set* do not suffer any internal reddening within M 31, while the others may, depending on their actual location. This choice,

Table 4. The samples of M 31 globular clusters.

Bo	G	sample°	Bo	G	sample°	Bo	G	sample°	Bo	G	sample°
1	39	1,2,3,4	40	102	1	77	139	1,2,3	113		3
2	43	1,2,3	41	103	1	78	140	1,2,3	114	175	1,2,3
3	45	1	42	104	1,2,3,4	79		3	115	177	1,2,3,4
4	50	1,2,3,4	43	106	1,2,3,4	80	141	1,2,3	116	178	1,2,3,4
5	52	1,2,3,4	44	107	1,2,3,4	81	142	1	117	176	1,2,3,4
6	58	1,2,3,4	45	108	1,2,3,4	82	144	1,2,3,4	118		1,2,3,4
7	59	1	46	109	1,2,3,4	83	146	1,2,3,4	119		1,2,3
8	60	1,2,3	47	111	1,2,3,4	84		1,2,3	123	182	1,2,3
9	61	1,2,3,4	48	110	1,2,3,4	85	147	1,2,3,4	124		1,2,3
10	62	1,2,3,4	49	112	1	86	148	1,2,3,4	125	183	1,2,3
12	64	1,2,3,4	50	113	1,2,3	88	150	1,2,3,4	126	184	1,2,3,4
13	65	1,2,3	51	114	1,2,3,4	89		1	127	185	1,2,3,4
15		1,2,3	53		1,2,3	90		3	128	187	1,2,3
16	66	1,2,3	54	115	1,3	91	151	1,2,3,4	129		1,2,3
17	70	1,2,3,4	55	116	1,2,3	92	152	1,2,3,4	130	188	1,2,3
18	71	1,2,3	56	117	1,2,3	93	155	1,2,3,4	131	189	1,2,3,4
19	72	1,2,3,4	57	118	1,2,3	94	156	1,2,3,4	132		3
20	73	1,2,3,4	58	119	1,2,3,4	95	157	1,2,3,4	133	191	1,2,3
21	75	1,2,3	59	120	1,2,3	96	158	1,2,3,4	134	190	1,2,3
22	74	1,2,3	60	121	1	97	159	1,2,3,4	135	192	1,2,3,4
23	78	1,2,3,4	61	122	1,2,3,4	98		1,2,3,4	136	194	1,2,3,4
24	82	1,2,3,4	63	124	1,2,3,4	99	161	1,2,3	138		1,2,3
25	84	1,2,3	64	125	1,2,3,4	100	163	1,2,3	141	197	1,2,3
26	86	1,2,3	65	126	1,2,3,4	101	164	1,2,3	143	198	1,2,3,4
27	87	1,2,3,4	66	128	1	102		1,2,3,4	144		1,2,3,4
28	88	1,2,3	67	129	1,2,3	103	165	1,2,3,4	145		3
29	90	1,2,3,4	68	130	1,2,3,4	104		1,2,3	146		1,2,3,4
30	91	1,2,3	69	132	1,3	105	166	1,2,3	147	199	1,2,3,4
31	92	1,2,3	70	133	1,2,3	106	168	1,2,3,4	148	200	1,2,3,4
33	95	1,2,3	71		1,2,3	107	169	1,2,3,4	150	203	1,2,3
34	96	1,2,3,4	72		1,2,3	108	167	1,2,3	151	205	1,2,3,4
35		1,2,3	73	134	1,2,3,4	109	170	1,2,3,4	152	207	1,2,3,4
36		1,2,3	74	135	1,2,3,4	110	172	1,2,3,4	153		1,2,3,4
38	98	1,2,3,4	75	136	1,2,3	111	173	1,2,3	154	208	1,2,3,4
39	101	1,2,3,4	76	138	1,2,3,4	112	174	1,2,3,4	155	210	1,2,3

© European Southern Observatory • Provided by the NASA Astrophysics Data System

quite arbitrary indeed, offers a practical procedure to exclude a few candidates from the final sample (see Sect. 8.1).

6.2. The "current best sample"

We thus define the "current best sample" of M 31 GCs as the sample which includes:

• *outside isophote No. 1* (de Vaucouleurs 1958)

a) All the candidates confirmed to be clusters via high-resolution imaging or spectroscopy (71 objects).

b) All the A+B candidates with $(B-V) \leq 1.10$ even if not confirmed via the quoted techniques (2 objects in total).

Note that we have discarded 8 clusters (*Bo31, G55, Bo331, Bo320, Bo324, Bo326, Bo329, Bo333*) as members to NGC 205.

• *inside isophote No. 1*

c) All the candidates confirmed to be clusters via high-resolution imaging or spectroscopy (138 objects).

d) All the A+B candidates even if not confirmed via the quoted techniques (152 objects in total, after the inclusion of the latest new candidates and the revision of the old classes discussed at Sect. 3), but excluding from this number 7 candidates (*Bo79, Bo90, Bo132, Bo145, Bo200, Bo264, BoD53*) as they are still lacking reliable colors, and 15 clusters (*Bo14, Bo32, Bo37, Bo52, Bo62, Bo122, Bo137, Bo149, Bo168, Bo191, Bo226, Bo305, Bo346, Bo388, Bo389*) having $(B-V) > 1.1$ and background parameter $bkg < 200$ (in our arbitrary units). Since this background threshold is very low and would not affect the intrinsic color significantly even if the object would be located behind it, we assume that these candidates are intrinsically redder than the reddest known cluster and are thus probably galaxies. We cannot exclude however that some of them might be very metal rich clusters (see Bica et al. 1992). This choice reduce from 152 to 130 the objects in this subset.

Note that we have discarded the 5 objects from ACH92 not included in our present compilation as we could not classify them properly.

In conclusion, the total number of objects included in the "current best sample" is 341. They are listed for clarity in Table 4. More specifically they include 247 A, 69 B, 15 C, 8 D and 2 objects non classified in *Bo-Group* (1987) because they were either too faint (*DAO 104*, Crampton et al. 1985; confirmed by Racine 1991), or out of field (*G3*, confirmed by Federici et al. 1993).

Of them 81 have been confirmed via high resolution imaging, 176 via spectroscopy, 48 via both methods.

7. The M 31 total cluster system: some speculations

There are two important questions one would like to answer when dealing with the M 31 cluster system, i.e. How large is the total globular cluster population? Is there any separation between disk and halo globulars? Both questions are hard to answer at the present stage of the study.

Table 4. (continued)

Bo	G	sample°	Bo	G	sample°	Bo	G	sample°	Bo	G	sample°
156	211	1,2,3	194	243	1,2,3	231	285	1,2,3	313	36	1,2,3
157	212	1,2,3	195		1	232	286	1,2,3,4	314	37	1
158	213	1,2,3,4	196	246	1,2,3	233	287	1,2,3,4	315	38	1,2,3,4
159		1,2,3	197	247	1,2,3	234	290	1,2,3	316	40	1,2,3
160	214	1,2,3	198	249	1,2,3	235	297	1,2,3,4	317	41	1,2,3,4
161	215	1,2,3,4	199	248	1,2,3	236	298	1,2,3,4	318	42	1,2,3,4
162	216	1,2,3	200		3	237	299	1,2,3	319	44	1
163	217	1,2,3,4	201	250	1,2,3,4	238	301	1,2,3,4	321	46	1
164		1,2,3	202	251	1	239		1,2,3,4	322	49	1
165	218	1,2,3,4	203	252	1,2,3	240	302	1,2,3,4	323		1,2,3
166		1,2,3,4	204	254	1,2,3,4	244		3	325		1,2,3,4
167		1,2,3	205	256	1,2,3,4	264		3	327	53	1,2,3,4
169		1,2,3	206	257	1,2,3,4	272		3	328	54	1,2,3,4
170	221	1,2,3	207	258	1,2,3	281	288	3	335		1,2,3
171	222	1,2,3,4	208	259	1,2,3	282		1	336	67	1,2,3,4
172	223	1,2,3	209	261	1,2,3,4	283	296	3	337	68	1,2,3,4
173	224	1,2,3	210		1	284		1,3	338	76	1,2,3,4
174	226	1,2,3,4	211	262	1,2,3,4	289		1,2,3,4	339	77	1,2,3,4
176	227	1,2,3,4	212	263	1,2,3,4	290		1,2,3,4	341	81	1,2,3,4
177	228	1	213	264	1,2,3,4	291	9	1,2,3,4	342	94	1
178	229	1,2,3,4	214	265	1,2,3	292	10	1,2,3,4	343	105	1,2,3,4
179	230	1,2,3,4	215	266	1,2,3	293	11	1,2,3,4	344	127	1,2,3,4
180	231	1,2,3,4	216	267	1,2,3,4	295	14	1,2,3,4	345	143	1,2,3,4
181	232	1,2,3	217	269	1,2,3,4	298	21	1,2,3,4	347	154	1,2,3
182	233	1,2,3,4	218	272	1,2,3,4	301	22	1,2,3,4	348	153	1,2,3
183	234	1,2,3,4	219	271	1,2,3,4	302	23	1,2,3,4	349		1,3
184	236	1,2,3	220	275	1,2,3,4	303	26	1	350	162	1,2,3,4
185	235	1,2,3,4	221	276	1,2,3,4	304	28	1,2,3,4	351	179	1,2,3,4
186		1,2,3	222	277	1	306	29	1,2,3,4	352	180	1,2,3,4
187	237	1,2,3	223	278	1	307	30	1,2,3	354	186	1,2,3
188	239	1,2,3	224	279	1,2,3,4	308		1	355	193	1,2,3
189	240	1,2,3	225	280	1,2,3,4	309	31	1,2,3,4	356	206	1,2,3,4
190	241	1,2,3	228	281	1,2,3,4	310	32	1,2,3,4	357	209	1,2,3,4
192	242	1	229	282	1,2,3,4	311	33	1,2,3,4	358	219	1,2,3,4
193	244	1,2,3,4	230	283	1,2,3,4	312	35	1,2,3,4	361	255	1,2,3,4

© European Southern Observatory • Provided by the NASA Astrophysics Data System

7.1. How many more M 31 globular clusters could exist and how detectable are they?

As frequently stressed, the study of both dynamical properties and chemical composition variations in M 31 would greatly benefit from the discovery of other cluster candidates, specially at large galactocentric distances.

After the repeated surveys carried out by many different groups, in the inner regions of M 31 (with $R < 10$ kpc) new candidates can probaly emerge only from searches of fainter objects (V > 18) or from the ability of detecting clusters rejected so far because their images are stellar (very compact clusters, mostly in the very central regions) or are very heavily reddened.

Turning to the outer regions, where the effects of internal reddening and background contribution are negligible, the number of known clusters can be useful in predicting the number of clusters which could actually be found by an appropriate search on wide field, high resolution images.

Figure 8 shows the distribution of globular clusters in our own Galaxy as a function of their galactocentric distance (in kpc), respectively for clusters brighter (Fig. 8a) and fainter (Fig. 8b) than $M_V = -6.5$, which corresponds to $V \sim 18$ at the M 31 distance. The data are from Webbink (1985). Figure 9 shows the distribution of all the M 31 globular clusters candidates included in our "current best sample" with a cut in magnitude (V=18) similar to that adopted in Fig. 8.

To extend further the analysis, one could then compare the M 31 distribution to the *projected* one for the Milky Way, using Eq. (5) quoted below, for instance. In Table 5, we report the results of this experiment made using for M 31 the sample of confirmed clusters or the "adopted best sample" (see Sect. 8).

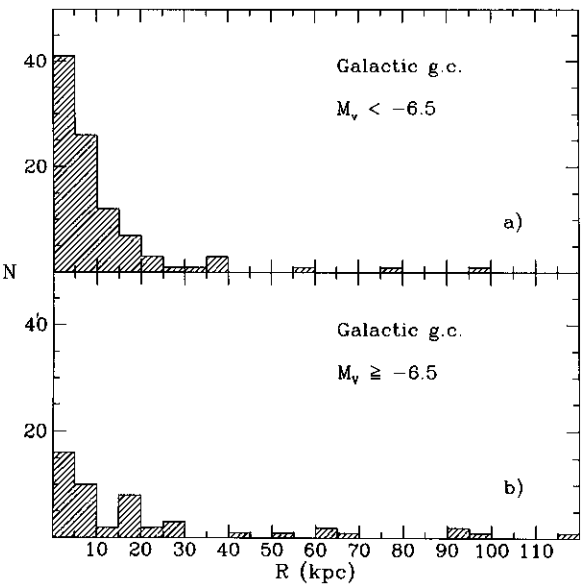

Fig. 8. Distribution of globular clusters in our own Galaxy as a function of their galactocentric distance (in kpc), respectively for clusters brighter (*a*) and fainter (*b*) than $M_v = -6.5$. The data are from Webbink (1985)

As can be seen from the table, the population ratios between M 31 and the Milky Way obtained from the data are quite strongly dependent on the sample used for M 31 and from the distance bin considered. In particular, the discrepancy obtained in the inner regions using the two different M 31 samples can easily be explained as due to the bias in the checking procedure applied to the candidate clusters. In fact, most of the high-resolution imag-

Table 4. (continued)

Bo	G	sample◇	Bo	G	sample◇	Bo	G	sample◇	Bo	G	sample◇
362		1,2,3	396	335	1,2,3,4	456		3		260	1,2,3,4
363	274	1,2,3,4	397	336	1,2,3,4	457	97	1,2,3,4		268	1,2,3,4
365	284	1,2,3,4	398	341	1,2,3	458		3		327	1,2,3,4
366	291	1,2,3,4	399	342	1,2,3,4	459		3		339	1,2,3,4
367	292	1	400	343	1,2,3,4	460		3		353	1,2,3,4
368	293	1	401	344	1,2,3,4	461	131	1,2,3,4	EXT8		1,2,3,4
370	300	1,2,3,4	402	346	1,2,3,4	462		1,3	NB16		1,3
371	303	1	403	348	1,2,3,4	463	160	3	NB17		1,3
372	304	1,2,3,4	405	351	1,2,3,4	467	202	1,2,3,4	NB18		1,3
373	305	1,2,3,4	407	352	1,2,3,4	468		1,2,3,4	D53		3
374	306	1	409		1,2,3,4	470		3	NB21		1,2,3
375	307	1,2,3,4	415		3	475		3	NB22		3
376	309	1,3	417		3	477		3	NB23		3
377	308	1,2,3,4	418		3	483		3	NB25		3
378	311	1,2,3	422		1,2,3,4	484	310	3	NB29		3
379	312	1,2,3,4	423		1,2,3,4	485		3	D54		3
380	313	1	425		3	486	316	1,2,3,4	NB42		3
381	315	1,2,3,4	426		1,2,3,4	491		3	D150		1,2,3,4
382	317	1,2,3	430	25	1,3	499		3	D167		1,2,3,4
383	318	1,2,3,4	431	27	1,2,3,4	500		3	D220		1,2,3,4
384	319	1,2,3,4	433		3	502		3	D225		1,3
385	321	1,2,3	436		3	505		1,2,3,4	D242		1,2,3,4
386	322	1,2,3,4	437		3	507		3	D337		1,3
387	323	1,2,3,4	443		3	510		3	D344		1,2,3,4
391	328	1,2,3	448		3		1	1,2,3,4	DAO 104 (*)		1,2,4
392	329	1,2,3,4	449		3		2	1,2,3,4			
393	330	1,2,3,4	450		1		3	1,2,3,4			

◇ 1 - "Current best sample" 2 - "Adopted sample" 3 - "Extended sample" 4 - "Confirmed sample"
(*) DAO Crampton et al.,1985 (Table 2)

© European Southern Observatory • Provided by the NASA Astrophysics Data System

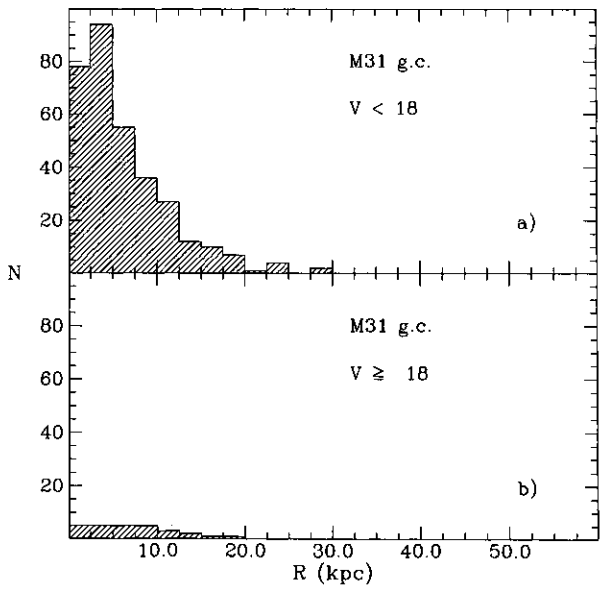

Fig. 9. Distribution of all the M 31 globular clusters candidates as a function of their galactocentric distance (in kpc), with a cut in magnitude at V=18, corresponding to $M_V = -6.5$ adopted in Fig. 8

Table 5. Comparison between the M 31 cluster radial distribution and the *projected* one for the Milky Way

R(Kpc)	N(R) M31*	M31†	MW°	M31*/MW	M31†/MW
0 - 5	76	152	54	1.4 ± 0.3	2.8 ± 0.4
5 - 10	56	75	22	2.5 ± 0.6	3.4 ± 0.8
10 - 15	33	35	9	3.7 ± 1.4	3.9 ± 1.5
15 - 20	19	19	6	3.2 ± 1.5	3.2 ± 1.5
20 - 25	4	4	2	2.0 ± 1.7	2.0 ± 1.7
	188	285	93	2.0 ± 0.3	3.1 ± 0.4

* confirmed sample
† 'adopted' best sample
◇ $M_V < -6.5$

ing and spectroscopic observations have preferentially picked up candidates located (or projected) outside the main body of M 31.

Limiting the comparison between the total populations of clusters in the two galaxies to a region where one can assume that both samples should be quite complete and uncontaminated, i.e. in the range 10-20 kpc, one gets:

$$N_{GC(M31)} \,/\, N_{GC(Galaxy)} = 52/15 \sim 3.5 \pm 1.0 \quad . \qquad (1)$$

Note that the ratio rises up to 3.6 if the "adopted best sample" is considered for M 31, while it decreases to $\sim 3.3 \pm 0.9$ if one adds also the bin 20-25 kpc. Using different approaches, Harris & Racine (1979) and Racine (1991) obtain for this ratio 2.5 ± 0.5 and 1.8 ± 0.3, respectively.

From the above considerations, it seems still quite difficult to derive a sufficiently precise ratio for the globular cluster populations in the two galaxies. However, assuming for sake of example 2.5±1.0 as most probable value (with a large, conservative uncertainty), and considering that outside 20 kpc there are in the Milky Way 12 clusters brighter than M_V=-6.5 and 13 fainter, one could expect to find about 30 clusters in M 31 brighter than V=18 and 33 fainter than that limit.

If one then restricts the comparison and estimates to the region between 20 and 30 kpc, already reached partially by the available surveys, there are 9 clusters (4 brighter than $M_V = -6.5$) in our own Galaxy and 6 in M 31, all brighter than $V = 18$ and spectroscopically confirmed. Hence, adopting the mean population ratio of 2.5, about 23 clusters are expected in M 31, 10 of which brighter than $V = 18$. Since 6 bright clusters have already been discovered in this area, one can expect to find 15-20 more clusters, mostly fainter than $V = 18$

Due to the low surface brightness expected for actual clusters at these galactocentric distances (Palomar-like objects are found in the Milky Way) and the large area to be scanned (~ 12 *sq.deg.*), the task of finding a few other clusters appears very difficult: for each square degree one has to check more than 1500 images to V=19.5 (~1000 stars, Allen 1985 and ~500 galaxies, Rainey 1977) in order to pick up about 1 globular cluster together with 2-3 misclassified galaxies morphologically and photometrically identical to globular clusters.

The game of detecting fainter candidates within 30 kpc or bright clusters in the outermost halo is of course still more challenging. The number of images to be inspected steeply increases with magnitude as does the area to survey going farther and farther away. Moreover, the incidence of sparse Palomar-like objects probably increases in M 31 too. To push further the search, we have secured a wide collection of plates with the Tautenburg Schmidt Telescope in order to pick up a new list of "optimal" candidates whose spectroscopic and high resolution scrutiny might eventually yield a small sample of confirmed clusters crucial to any real quantitative step in these type of studies.

7.2. Disk and halo clusters

A second aspect which should be quantitatively clarified before studying the $\Sigma - R$ law for the M 31 GCs (see Sect. 9), is the separation between clusters belonging to different components within the galaxy.

It is now widely accepted (Zinn 1985,1986) that the GCS in the Milky Way can be divided into two main families, the disk and halo globulars. If a similar situation holds for the M 31 GCS, most of the clusters projected on the M 31 bulge or outside the disk should belong to the "spheroidal" component but a good fraction of those projected on the disk could be "disk" globulars, or even bright open clusters. This could have an important impact on the deduced $\Sigma - R$ relation, specially if the number of disk globulars were high compared to the halo one. In particular, this fact would raise Σ above the true spheroidal profile at intermediate R.

The problem of the existence of different subsystems in the M 31 GC's has been repeatedly discussed (van den Bergh 1969; Freeman 1983; Searle 1984; Elson & Walterbos 1988; Huchra et al. 1991; Racine 1991). There is some evidence from the kine-

© European Southern Observatory • Provided by the NASA Astrophysics Data System

matics that, as in the Milky Way, the GC's in M 31 constitute two main subsystems: a rotating thick disk of metal rich clusters and a spherical system of metal poor objects. Moreover, Elson & Walterbos (1988) point out that 14 of the 159 clusters in their sample could be young ($< 10^9 yr$). If this were confirmed by future studies, the incidence of "spurious" clusters could significantly bias the $\Sigma - R$ relation for the spheroidal component.

A quantitative analysis of the discrimination of the clusters with respect to the possible components within M 31 requires the consideration of many parameters (positions, kinematics, metallicity,..) for each cluster. We are currently assembling this data-set and postpone this part of the discussion to the future global paper (Battistini et al. 1993, in preparation). However, we add a few more considerations to get from the "current best sample" the "adopted one" to eliminate at least the contribution of the "young" globulars already identified and to reduce to a minimum the possible effects due to a residual lack of homogeneity still present in the "current best sample" defined in Sect. 6 (see Table 4).

8. The "adopted best sample"

Since, as mentioned at Sect. 5.3, in the very central regions and in part of the outer halo either the search for cluster candidates or the check of their intrinsic nature have been extended to a deeper magnitude limit than elsewhere, we should introduce an homogeneous limiting magnitude threshold.

In particular, in the outer regions we limit the sample to clusters brighter than V $\sim$ 18.0. This leads to exclude from the "current best sample" presented at Sect. 6 and listed in Table 4, 8 clusters (*Bo282, Bo284, Bo430, Bo450, Bo462, BoD225, BoD337, DAO104*).

Concerning the central regions, the definition of the magnitude threshold is made more difficult by extinction. In fact, intrinsically bright clusters may appear fainter due to high reddening. As a compromise between the need of cutting the faint tail (undetected in the other regions) and keeping bright reddened clusters, we have chosen to include in the *inner sample* the clusters brighter than $V = 18.0$, thus eliminating 2 objects from the "current best sample" (*Bo 69, Bo376*).

The final problem is to separate young and disk clusters from the "true" halo globulars.

To eliminate clusters which probably belong to a "young" population (open clusters or blue globulars, like in the Magellanic Clouds), we reject from the "current best sample" (Sect. 6) objects bluer than $B - V \leq 0.58$ since the bluest globular cluster in the Milky Way has $(B - V)_o = 0.52$ (NGC 7492, Webbink 1985) and the minimum reddening estimated in the M 31 region of the sky is E(B-V) = 0.06 (Bica et al. 1992).

Recalling how the "current best sample" was built in Sect. 6 and after introducing these further constraints, the "adopted best sample" is defined as follows:

- outside isophote No. 1

a) All the candidates confirmed to be clusters via high-resolution imaging or spectroscopy with V $\leq$ 18.0 (63 objects).

b) All the A+B candidates with $0.58 \leq (B - V) \leq 1.10$ even if not confirmed via the direct de-contaminating techniques, but with V $\leq$ 18.0 (2 objects in total).

- inside isophote No. 1

c) All the candidates confirmed to be clusters via high-resolution imaging or spectroscopy with V $\leq$ 18. (136 objects).

d) All the A+B candidates with $(B - V) \leq 0.58$ and V $\leq$ 18. even if not confirmed via the quoted techniques (105 objects in total, after the inclusion of the latest new candidates and the revision of the old classes discussed at Sect. 3).

In conclusion, the 298 objects included in the "adopted best sample" and specifically marked for clarity in Table 4 are 233 A, 48 B, 10 C, 6 D and 1 object not classified in *Bo-Group* (1987). Of them, 199 are confirmed, 72 by high resolution imaging, 174 by spectroscopy, 47 by both methods.

9. The projected number density of the globular cluster system in M 31

Globular cluster systems in galaxies can be described by the number of clusters at the projected radius R. This function, the so–called projected number density, is defined as $\Sigma(R) = dN(R)/dA(R)$ [where $dA(R)$ is the area of the circular annulus at the projected galactocentric distance R which has been surveyed, and $dN(R)$ is the number of objects contained therein]. It has traditionally been represented analytically using either a power–law (i.e. R^{-n}–law) or a de Vaucouleurs law (i.e. $R^{1/4}$–law).

As is well known, the degree of success of the $R^{1/4}$–law in fitting observations of surface brightness in ellipticals and bulge of spirals is high. Consequently, the main incentive to adopt a $R^{1/4}$–law stems from the aim of verifying whether Σ for the cluster system and for the surface brightness profile of the spheroidal component of the parent galaxy are coextensive, i.e. have the same scale factor. This knowledge would have a strong impact on the study of galaxy formation and early evolution (Harris 1987, and references therein).

However, it is not evident that the $R^{1/4}$–law is superior to the power–law in describing the cluster distribution. De Vaucouleurs (1977) argues that *it is obvious that the distributions are nonlinear in the (Log Σ, LogR) plane and, consequently, that the power–laws are at best merely interpolation formulas applicable over a small range of distances and densities.* But the question whether there is a clear–cut physical property which privileges the $R^{1/4}$–law among all the $R^{1/m}$–relations is still matter of debate even in the description of the surface brightness of elliptical galaxies (see for instance Makino et al. 1990). A deeper analysis of these aspects is however beyond the purposes of the present Note. In any case it may be hard to justify *a priori* on physical grounds why, in particular, people study the *flattening* of the projected number density profiles of the globular cluster system of M 31 with respect to the predictions of the $R^{1/4}$–law rather than with respect to other analytical representations.

© European Southern Observatory • Provided by the NASA Astrophysics Data System

Based on the "adopted best sample" of M 31 globular clusters, in the following paragraphs we:

(1) Determine the "observed" effective radius $-R_e-$ of the M 31 cluster system.
(2) Compute the best fitting parameters assuming the $R^{1/4}$–law.
(3) Compute the best fitting parameters m for the $R^{1/m}$–law and n for the R^{-n}–law, and discuss which is the best fitting law.
(4) Verify how the exclusion or inclusion of candidates (at different level of confidence) modifies the measured physical scales (particularly the effective radius of the system) with the $R^{1/4}$–law and how sensitive the values of m and n are to the variations of the data-set.
(5) After imposing the validity of the obtained $R^{1/4}$–law computed using only the clusters outside a fixed projected galactocentric distance (3,2,1 kpc), verify whether there is still a residual central flattening with respect to the inner extrapolation of the best fitting solution, and study how the addition of further candidates (of lower and lower confidence) would eliminate it, setting also an upper limit to the number of the *possible* cluster candidates in the area (down to V$\simeq$19.0).

To carry out the following computations, the "adopted best sample" (see Table 4) has been divided into bins going from galactocentric projected distance of 1 kpc out to 29 kpc with step of 1 kpc. The inner regions have been split into three smaller bins ranging respectively from 0.1 kpc to 0.3 kpc, from 0.3 kpc to 0.5 kpc, and, finally, from 0.5 kpc to 1.0 kpc. The central region (R <0.1 kpc) has been discarded. Two quantities have been computed in each considered annulus: the arithmetic mean radius of the objects here contained, $< R >$, and the corresponding projected number density, $\Sigma(< R >)$ (see Table 6).

9.1. Error bars and fitting procedures

The actual errors affecting the values listed in Table 6 for $\Sigma(< R >)$ are difficult to be estimated correctly. In fact, besides the usual statistics, they depend essentially on the uncertainties linked to the procedure of selection and de-contamination of the available sample. In the following paragraphs, we adopt for sake of example the error bars resulting from adopting $\sigma_{\Sigma(R)} = \sqrt{N(R)}/A(R)$. It is thus quite obvious that when the counts are small and/or the area is large the error bars are strongly amplified in the $log-$ (see Fig. 10).

The uncertainties affecting the proper estimate of the errors affect also the choice of the best fitting procedure. In particular, we anticipate that in the various cases we are going to discuss the use or not of specific weights may alter the results accordingly.

To understand better this last item we have carried out some tests. Schematically, in the procedure used to estimate the best

Table 6. Projected density distributions of GC's in the various M 31 samples.

"adopted best sample"				"extended sample"				"confirmed g.c. sample"			
R(Kpc)	N(R)	Σ(R)	$< R >$	R(Kpc)	N(R)	Σ(R)	$< R >$	R(Kpc)	N(R)	Σ(R)	$< R >$
.1 - .3	3*	15.45†	0.24	.1 - .3	5*	25.75†	0.25	.1 - .3	1*	5.15†	0.28
.3 - .5	4◇	9.55†	0.45	.3 - .5	9◇	21.38†	0.43	.3 - .5	2◇	4.68†	0.45
.5 - 1	8○	7.94†	0.78	.5 - 1	13○	12.88†	0.81	.5 - 1	6○	6.03†	0.78
1 - 2	37	3.93	1.50	1 - 2	38	4.03	1.49	1 - 2	17	1.80	1.54
2 - 3	34	2.16	2.53	2 - 3	37	2.36	2.53	2 - 3	18	1.15	2.57
3 - 4	32	1.46	3.44	3 - 4	34	1.55	3.45	3 - 4	19	0.86	3.44
4 - 5	34	1.20	4.46	4 - 5	38	1.34	4.47	4 - 5	13	0.46	4.44
5 - 6	19	0.55	5.38	5 - 6	21	0.61	5.39	5 - 6	14	0.41	5.36
6 - 7	16	0.39	6.56	6 - 7	17	0.42	6.57	6 - 7	14	0.34	6.52
7 - 8	12	0.25	7.50	7 - 8	14	0.30	7.50	7 - 8	8	0.17	7.41
8 - 9	15	0.28	8.52	8 - 9	22	0.41	8.55	8 - 9	10	0.19	8.51
9 - 10	13	0.22	9.56	9 - 10	16	0.27	9.55	9 - 10	10	0.17	9.50
10 - 11	9	0.14	10.46	10 - 11	11	0.17	10.41	10 - 11	9	0.14	10.46
11 - 12	10	0.14	11.47	11 - 12	12	0.17	11.47	11 - 12	9	0.12	11.52
12 - 13	8	0.10	12.32	12 - 13	9	0.11	12.39	12 - 13	7	0.09	12.27
13 - 14	3	0.04	13.67	13 - 14	5	0.06	13.73	13 - 14	3	0.04	13.67
14 - 15	5	0.05	14.47	14 - 15	7	0.08	14.50	14 - 15	5	0.05	14.47
15 - 16	4	0.04	15.39	15 - 16	6	0.06	15.47	15 - 16	4	0.04	15.39
16 - 17	9	0.09	16.64	16 - 17	11	0.11	16.64	16 - 17	9	0.09	16.64
17 - 18	2	0.02	17.35	17 - 18	4	0.04	17.52	17 - 18	2	0.02	17.35
18 - 19	4	0.03	18.49	18 - 19	5	0.04	18.41	18 - 19	4	0.03	18.49
19 - 20	0			19 - 20	1	0.01	19.17	19 - 20	0		
20 - 21	1	0.01	20.99	20 - 21	1	0.01	20.99	20 - 21	1	0.01	20.99
21 - 22	1	0.01	21.98	21 - 22	3	0.02	21.40	21 - 22	1	0.01	21.98
22 - 23	1	0.01	22.61	22 - 23	2	0.01	22.39	22 - 23	1	0.01	22.61
23 - 24	1	0.01	23.95	23 - 24	1	0.01	23.95	23 - 24	1	0.01	23.95
24 - 25	0			24 - 25	0			24 - 25	0		
25 - 26	0			25 - 26	0			25 - 26	0		
26 - 27	0			26 - 27	0			26 - 27	0		
27 - 28	0			27 - 28	0			27 - 28	0		
28 - 29	2	0.01	28.48	28 - 29	2	0.01	28.48	28 - 29	2	0.01	28.48

Notes to Table 5:
* area surveyed = 5.40 arcmin^2, total area = 6.99 arcmin^2
◇ area surveyed = 11.76 arcmin^2, total area = 13.98 arcmin^2
○ area surveyed = 27.92 arcmin^2, total area = 65.50 arcmin^2
† obtained dividing the number counts by the area surveyed (in Kpc^2)

© European Southern Observatory • Provided by the NASA Astrophysics Data System

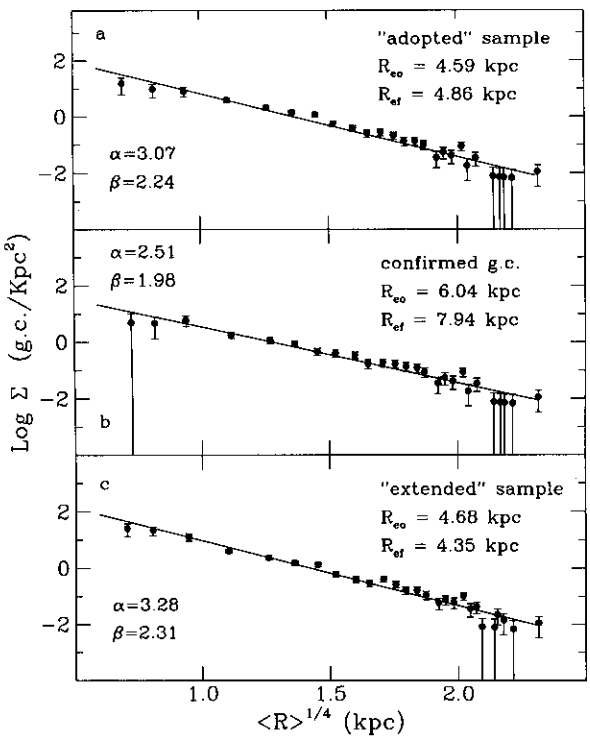

Fig. 10. Best fitting $R^{1/4}$–law for the various samples discussed in the text (Sect. 9). R_{eo} is the observed effective radius computed on the sample, R_{ef} is the corresponding value computed from the best fit. Error bars: see discussion in the text

fitting parameters in the various analytical representations we are going to use with the various data samples, we have required that the quantity $s = \sqrt{\sum_{i=1}^{N}(C-O)^2/w^2(N-1)}$ has a minimum. In this expression w is a weight which in the tests we made may be equal to 1, σ_Σ, σ_Σ/Σ. In essence, $w = 1$ implies that each bin has the same weight; $w = \sigma_\Sigma/\Sigma$ gives much higher weight to the bins where the *relative* error on Σ is smaller; $w = \sigma_\Sigma$ assigns a weight controlled by the variation of *absolute* error on Σ.

The results of the tests show that, for any considered sample, the adoption of weights depending on the *relative* errors sistematically increases the importance of the inner bins, leading for instance to unreliably high values for the fitted *effective* radius (see Sect. 9.2) and very flattened overall profiles.

On the other hand, the use of weights related to the *absolute* errors (rather than $w = 1$) does not affect strongly the results obtained by fitting the data with the $R^{1/4}$–law and, in general, with the $R^{1/m}$–law, whilst it leads to much steeper fittings if a R^{-n}–law is used. In particular, the value of the best fitting n can even be twice as much as the one obtained with $w = 1$, thus increasing in practics the weight of the outer bins.

Though we stress here the importance of getting a deeper insight on this specific problem, since we do not have at this stage any clear-cut reason to assign a different weight to the various radial bins, we have chosen to set $w = 1$ throughout all the following analysis and discussion.

9.2. Fitting the $R^{1/4}$–law

Once the "adopted best sample" is defined, it is immediate to determine the *observed* value of the *effective radius*, R_{eo}, defined as the median distance for the cluster population. We find $R_{eo} = 4.65$. If we take into account that a small fraction of the central areas has not been surveyed yet, and normalize to the total, R_{eo} decreases to 4.59 kpc.

Assuming that the projected number density Σ follows the $R^{1/4}$–law, we can then obtain the *effective fitted* physical scales Σ_{ef} and R_{ef} by a mean least square fit of the two parameters α and β, that determine the relation

$$\mathrm{Log}\Sigma = \alpha - \beta < \mathrm{R} >^{1/4} . \qquad (2)$$

In particular, the parameter β is related to R_{ef} via the formula $R_{ef} \simeq (3.33/\beta)^4$, and so any variation of β produces very large changes in the value of R_{ef}.

The plot of LogΣ versus $< R >^{1/4}$ for the "adopted best sample" is shown in Fig. 10a. In the diagram, the straight line represents the *best fitting* $R^{1/4}$–law. In Fig. 10a are also reported the *fitted* R_{ef} and the corresponding *observed* R_{eo}.

A proper interpretation of the result presented in Fig. 10a and of the comparison of the fitted and observed values of the effective radius – R_{eo} and R_{ef} – requires however some preliminary considerations. In fact, the conclusions one may draw are different depending on the actual completeness and degree of radial bias present in the considered sample.

If the "adopted best sample" is *complete*, or at least contains no radial bias, one has two possibles alternatives:

a) If $R_{eo} = R_{ef}$, then the $R^{1/4}$–law is fully compatible with the data distribution. However, this would not be sufficient to exclude that a different law could match the data even better.

b) If $R_{eo} \neq R_{ef}$, then one is forced to conclude that the adopted $R^{1/4}$–law can hardly describe properly the observations, but this does not seem to be the actual case.

Were the "adopted best sample" *incomplete*, or radially biased, a discrepancy between R_{eo} and R_{ef} would not be sufficient to exclude the validity of the $R^{1/4}$–law. The addition of further data to eliminate the radial bias would of course be the only way to improve the analysis.

Note that adding new objects in the central regions, decrease both the *fitted* and the *observed* effective radii. Note also that R_{ef} decreases much more steeply than R_{eo}. Since R_{ef} is inversely proportional to the fourth power of the slope of the fit, R_{ef} is highly sensitive to small variations of this number: great variations of R_{ef} need not correspond to real variations of R_{eo}. Therefore, it is evident that R_{ef} is more a measure of the slope of the globular cluster distribution than a significative measure of the true R_e of the sample. The use of the *fitted* quantities as the *true* physical parameters in discussions concerning the dynamics and the evolution of globular cluster system may thus be hazardous.

© European Southern Observatory • Provided by the NASA Astrophysics Data System

9.3. Other fitting formulae

Given the above results and considerations, it is quite natural to examine different formal approaches to describe the globular cluster distribution. In particular, one can measure directly from the data R_{eo} and Σ_{eo} –the observed projected number density, and then fit the normalized distribution as a function of the normalized radius. We have tested how relations, like

$$\frac{\Sigma}{\Sigma_{eo}} = \exp\{-b(m)[(R/R_{eo})^{1/m} - 1]\}, \quad (3)$$

[where $b(m) \simeq 2m - 0.324$, Ciotti 1991], and

$$\frac{\Sigma}{\Sigma_{eo}} = \left(\frac{R}{R_{eo}}\right)^{-n}, \quad (4)$$

fit the adopted best sample. The best fitting solutions obtained are shown in Fig. 11a,b.

Table 7 shows that the best value for m is < 4 and ~ 1.6. We find that s is very sensitive to the change of the exponent (see Fig. 12), a strong indication that the $R^{1/4}$–law as expressed in Eq. (3) is not the best fitting law for our considered sample. If our "adopted best sample" is unbiased, the *spatial* distribution of the globular clusters in the central regions of M 31 is approximated by $\sim r^{-1/2}$ (Ciotti 1991), which is much flatter than the behaviour $r^{-3/4}$, typical of the $R^{1/4}$–law (Young 1976).

The results obtained by fitting the data with the R^{-n} laws are worse (see Fig. 11b). This can easily be understood since the $R^{1/m}$–law is well fitted by an appropriate composition of two R^{-n} profiles (Makino et al. 1990). This is the reason why in the intermediate region of the distribution the data in the (Log$R$,LogΣ)–plane are underestimated by the best, single–slope fit based on an R^{-n}–law.

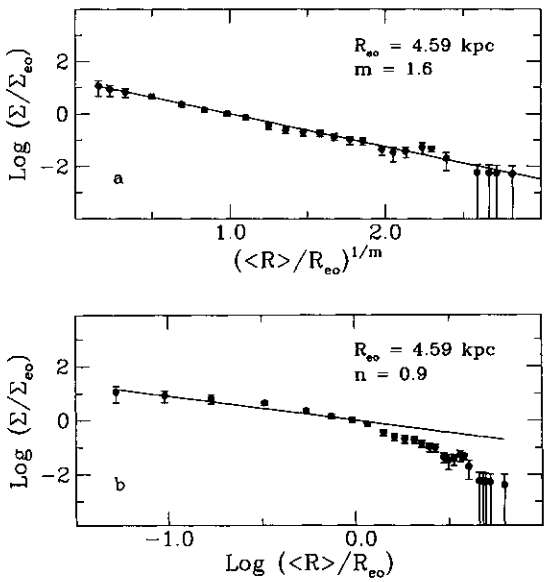

Fig. 11. Best fitting $R^{1/m}$–law and R^{-n}–law for the "adopted best sample". Error bars: see discussion in the text

Finally, we note that the same fitting procedures applied to the M 31 cluster data in luminosity do not lead to any significant variation of the results (see Table 7).

9.4. If alternative "plausible" samples were adopted: how do the results vary?

In the previous two paraghraphs we have obtained the best possible values for the main parameters describing the cluster density profile based on the "adopted best sample". Independently of

Table 7. The parameters of the best fitting $R^{1/m}$–law and R^{-n}–law for the three subsamples.

	g.c. sample	R_{eo} (Kpc)	Σ_{eo} (g.c./Kpc^2)	m	s	n	s
M31							
	'adopted'	4.59	1.31	1.6	0.18	0.9	0.75
	'extended'	4.68	1.41	2.2	0.63	1.1	1.64
	confirmed g.c.	6.04	0.40	2.4	0.42	1.2	0.84
Galaxy							
	($M_V < -6.5$)	4.41	0.36	1.9	0.32	1.3	0.48
	g.c. sample	RL_{eo} (Kpc)	ΣL_{eo} ($L_{V\odot}$/Kpc^2)	m	s	n	s
M31 (luminosity)							
	'adopted'	4.57	1944	2.2	3.06	1.1	2.02
	'extended'	4.62	1908	2.3	3.20	1.1	2.21
	confirmed g.c.	4.99	1013	2.4	3.03	1.1	2.41

R_{eo}, Σ_{eo} = "observed" effective radius and projected number density, directly derived from the g.c. distribution.
RL_{eo}, ΣL_{eo} = "observed" effective radius and projected number density, directly derived from the g.c. distribution in luminosity.

© European Southern Observatory • Provided by the NASA Astrophysics Data System

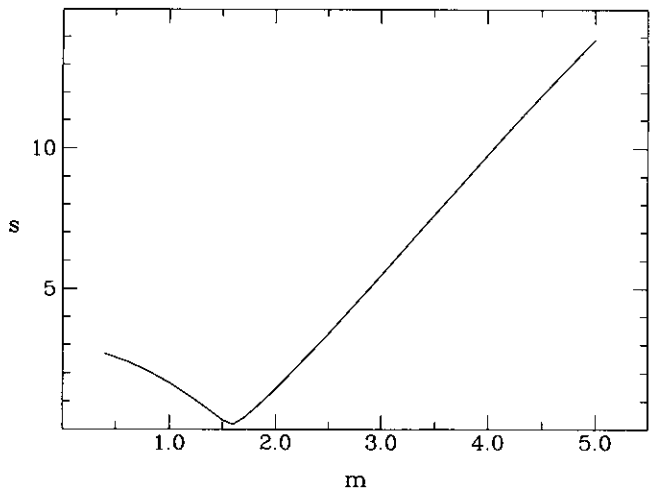

Fig. 12. $s-$values with varying m in fitting the $R^{1/m}$–law

the adopted law, it is however important to estimate the systematic errors which might be associated to these values. A reliable way of getting such estimates is to see how much these values depend on the adopted sample. In particular, one can determine how they change by varying the sample between two extreme cases.

The first, by adopting as basic sample that formed by all the "confirmed" clusters only, i.e. the 199 candidates whose cluster nature has been directly confirmed via spectroscopy and/or high-resolution imaging (see the remarks in Table 4). This is the smallest (but also the more conservative) sample of M 31 clusters. Note that it has some intrinsic bias due to the non homegeneous survey of the candidates.

The second, by adding to the "adopted best" sample also the candidates listed in the C-class by *Bo-Group* (1987) whose nature has not been directly checked yet, but which satisfy the conditions in positions and colors set in Sect. 8, and extending the cut in magnitude down to V=18.5 since C-class candidates are generally fainter than those in the A,B classes. Finally, a few other candidates could be recovered for various reasons.

This first extension adds 25 C-candidates in the *inner set* and 13 in the *outer set*, respectively. In addition, 13 A,B clusters fainter than V=18.0 are now included. Finally, we reintroduce the 7 A,B candidates deleted from the "current best sample" because they still lack sufficient photometric information.

In total this second sample, hereafter called "the extended sample" (see remarks in Table 4), is actually *the largest sample of M 31 candidates having a sufficiently reliable degree of confidence*. It includes 356 objects. Although inferior to that of the "best" sample, its degree of homogeneity and completeness should be still fairly good, and thus its use is in our view sufficiently meaningful.

Table 8 summarizes the status and the actual number of objects listed in the various samples considered here.

By repeating the whole procedure described in Sect. 9.1 and 9.2, we obtain the results reported in Fig. 10b,c and Table 7, respectively, and which can be compared with the corresponding ones obtained from using the "adopted best sample" (Fig. 10a).

Table 8. The samples of M 31 cluster candidates considered in the present paper (see Sect. 6.2, 8, and 9.3).

	A	B	C	D	not class.	Total
"current" best sample	247	69	15	8	2	341
"adopted" best sample	233	48	10	6	1	298
"confimed" g.c.	161	21	10	6	1	199
"extended" best sample	239	56	51	8	2	356

As can be seen, while the consideration of just the confirmed clusters leads to very different results, the use of the "extended sample" does not vary significantly the values of the parameters found based on the "adopted best sample". From this one could draw the following considerations:

1. The available best samples of M 31 cluster candidates specifically treated to minimize the effects of contamination, non-homogeneity, and incompleteness down to a fixed magnitude limit, seem to be sufficiently unbiased to yield a "stabilized" overall trend for the description of their projected number density.
2. The agreement between the "observed" and "fitted" parameters indicates that the $R^{1/4}$–law is suitable to describe the projected number density profile, *though it is not necessarily the best fitting law*. An $R^{1/m}-$law, with m =1.6 yields a better fit to the data (see Eq. (3) and Fig. 12).
3. The consideration of the "confirmed" clusters only leads to a much shallower distribution, but it surely suffers from the bias still affecting the confirming procedure. To avoid background contamination within M 31 itself, most of the spectroscopic and high resolution observations have been carried out in the outskirts of the galaxy. This has introduced a radial bias which results in a predominant weight of the outer clusters.

A last point to mention again is the problem of the separation between disk and halo clusters. We have discarded from the "adopted sample" all clusters bluer than B–V=0.58. However, if the dynamical evolution of the M 31 cluster system resembles that for the Milky Way (Zinn 1985,1986), many clusters projected on the disk could actually be "disk globulars" rather than "true halo globular clusters". A correct evaluation of this effect can be done only after examining specifically the complete data set for each individual object for kinematical properties and chemical abundances. Such a global effort is in progress and a wealth of information is contained in studies under publication. We thus postpone the analysis to a future paper (Battistini et al. 1993, in preparation).

9.5. If the $R^{1/4}$–law is assumed: is there any residual flattening?

As reported in the Introduction, there has been a quite wide debate about the possible existence of a *flattening* of the cluster density profile with respect to the $R^{1/4}$–law in the central regions of M 31. This question was the origin of the search for candidates presented here. In the previous Sections however we

© European Southern Observatory • Provided by the NASA Astrophysics Data System

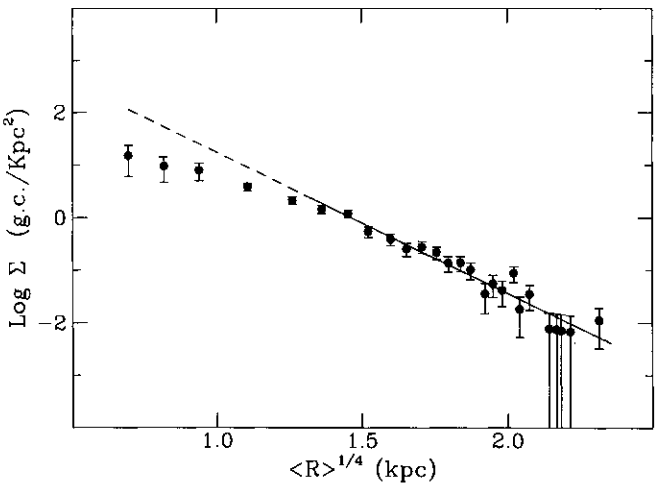

Fig. 13. Best fitting $R^{1/4}$–law (excluding the objects with r < 3kpc) and the residual "central flattening"

have discussed the issue in a more general way, trying first to determine the best description of the best available sample and even abandoning the assumption of a $R^{1/4}$–law.

It is still interesting to verify whether, after imposing the validity of the $R^{1/4}$–law defined by the parameters deduced by using exclusively the clusters projected outside a fixed galactocentric distance, there is still a *flattening* of the distribution after the addition of our new candidates. Moreover, since we have a complete list of the objects located in that area, with different degree of confidence as to their classification as clusters, it is interesting to see how many need to be "clusters" to totally eliminate this effect. This may be important to evaluate the impact of cluster distruction and survival.

In Fig. 13 we show how the best fitting $R^{1/4}$–law computed using the clusters outside 3 kpc from the nucleus (solid line) would be extrapolated (dotted line) in the inner regions. As can be seen from the Fig. 13 and Table 9, one would need 261 clusters with R <3 kpc to match the fit up to the center. This figure is about 2.5 times larger than the actual number of objects detected in this area and listed in the "adopted best sample".

To clarify the situation better, we give in Table 9 how the number of clusters expected within 3 kpc from the M 31 center varies with the sample considered or with the galactocentric distance (from 3 kpc to 2 and then 1) to which the fit has been computed and inside which the trend has been extrapolated. As can be expected, the size of "residual flattening" decreases significantly when the extrapolating distance is reduced, but it remains unless one also includes in the sample all the D-class candidates with "appropriate" colors (20 with V<18.5 and B-V>0.58) and even a fraction of the objects which have been discarded as "stars".

On the other hand, Fig. 10 also suggests the existence of a *steepening* in the outer regions whose explanation can be ascribed to incompleteness, but it could well be real. As already noticed by Racine (1991), independently of the adopted law, it is quite evident that the number density of M 31 clusters yielded by the available samples falls at galactocentric distances larger than R >20 kpc. About 20 candidates would be lacking according to the Racine's estimate. Judging from our survey (*Bo–Group*), we are inclined to believe unlikely the detection of many other good candidates in the annulus 20 < R < 30 kpc where the *outer steepening* is apparent. Hence, *it may be that in M 31 as in the Milky Way the spheroidal halo of bright globular clusters effectively ends at R ~40 kpc* (Racine 1991).

10. Comparison with our own Galaxy

Before closing, it is interesting to compare the results for M 31 with those for our own Galaxy, and to compare the distribu-

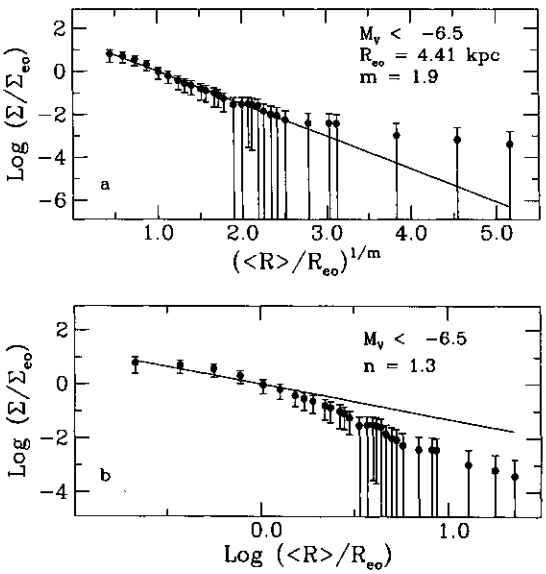

Fig. 14. The projected globular cluster system of the Galaxy fitted with a $R^{1/m}$–law *(a)*, and with a R^{-n}–law *(b)*. Error bars: see discussion in the text

Table 9. The problem of the residual "central flattening" with respect to the $R^{1/4}$–law.

	g.c. detected	g.c. normaliz.(*)	g.c. predicted inside 3 Kpc ($R^{1/4}$ >3Kpc)	($R^{1/4}$ >2Kpc)	($R^{1/4}$ >1Kpc)
"adopted best sample"	99	99	261	223	180
"extended sample"	116	123	258	221	180
"confirmed g.c. sample"	54	53	250	214	175

39 class D-candidates with R > 3 Kpc, 20 of them have V<18.5 and (B-V)≥ .5
91 "stars", 69 of them have V<18.5 and (B-V)≥ .5

* normalized to the total central area

© European Southern Observatory • Provided by the NASA Astrophysics Data System

tion of the globular clusters with the photometric profiles of the spheroidal components.

To carry out these comparisons, we have projected the spatial distribution of the globular clusters with M_V <–6.5 in the Galaxy (Webbink 1985) using the well–known formula based on the assumption of spherical symmetry:

$$\Sigma(R) = 2 \int_R^{R_t} \frac{n(r) r dr}{\sqrt{r^2 - R^2}}. \quad (5)$$

Then we have fitted with $R^{1/m}$ and R^{-n} laws the projected number density obtained, after fixing the measured R_{eo} and Σ_{eo} as was done in Sect. 9.2.

The values of m and n obtained for the best fits are 1.9 and 1.3, respectively (Table 7), i.e. *nearly the same* as for M 31 (see Fig. 14 and Fig. 11).

Finally, we note that the R_e–value for the optical halo formed by the stellar spheroidal component of the parent galaxy is probably smaller than that of the globular cluster system both in M 31 and in the Galaxy (Harris 1987, 1991, and references therein).

If confirmed, this might suggest that the globular cluster systems are older than the bulk of the surrounding halos, but further data are necessary before drawing such a strong conclusion.

Acknowledgements. We are indebted to W.E. Schoening and D.H. Hamilton for the loan of two excellent 4m KPNO plates. Thanks are also due to the staff of the Loiano telescope for help provided during observations, and to Dr. M. Lolli for advice with the MIDAS package. Finally, it is a pleasure to thank Dr. R. Racine, the referee, who suggested to us how to significantly improve the whole study. This research has been supported by the *Gruppo Nazionale di Astronomia* of the *Consiglio Nazionale delle Ricerche* and by the *Ministero dell' Università e della Ricerca Scientifica e Tecnologica.*

References

Allen, C.W. 1985, Astrophysical Quantities, The Athlone Press, London and Dover, p.243
Alloin, D., Pelat, D., Bijaoui, A. 1976 A&A, 50, 127
Aurière, M., Coupinot, G., and Hecquet, J. 1992, A&A, 256,95 (ACH92)
Baade, W., Arp, H.C. 1964, ApJ, 139, 1027
Bahcall, J.N., Soneira, R.M.:1980, ApJS, 44, 73
Battistini, P., Bònoli, F., Braccesi, A., Fusi Pecci, F., Marano, B. 1980, A&AS, 42, 357 *Bo-Group*
Battistini, P., Bònoli, F., Braccesi, A., Federici, L., Fusi Pecci, F., Marano, B., Borngen, F. 1987, A&AS, 67, 447 *Bo-Group*
Battistini, P. et al. 1993, in preparation
Battistini, P., Guarnieri, M.D. 1985, Astronomical catalogs in the M 31 region, in: Convegno ASTRONET, ed. G, Sedmak, Mem. Soc. astr. ital., p. 333
Bica, E., Jablonka, J.F.C., Santos, Jr., Alloin, D., and Dottori, H. 1992, A&A, 260, 109
Buonanno, R., Corsi, C.E., Battistini, P., Bònoli, F., Fusi Pecci, F. 1982, A&AS, 47, 451
Bystedt, J.E.V., Brinks, E., de Bruyn, A.G., Israel, F.P., Schwering, P.B.W., Shane, W.W., Walterbos, R.A.M. 1984, A&AS, 56, 245
Christian, C.A., and Heasley, J.N. 1991, AJ, 101, 848
Ciotti, L. 1991 A&A, 249, 99
Cohen, J.G., Freeman, K.C. 1991, AJ, 101, 483
Collura, A., Reale, F., Peres, G. 1990, ApJ, 154, 891
Crampton, D. 1984, in: X-Ray Astronomy '84, eds. Minoru Oda and R. Giacconi, Institute of Space and Astronomical Science, p. 403
Crampton, D., Schade, D.J., Chayer, P. and Cowley, A.P. 1985, ApJ, 288,494
Elson, R.A.W., Walterbos, R.A.M. 1988, ApJ, 333, 594
Federici, L., Fusi Pecci, F., Marano, B. 1990, A&A, 236, 99
Federici, L., Bònoli, F., Ciotti, L., Fusi Pecci, F., Marano, B., Lipovetsky, V.A., Neizvestny, S.L., and Spassova, N. 1993, A&A, in press
Ford, H.C., Jacoby, G.H.:1978, ApJS, 38, 351
Freeman, K.C. 1983, in: Internal Kinematics and Dynamics of Galaxies, ed. E. Athanassoula, Reidel, Dordrecht, p. 359
Frogel, J.A., Persson, S.E., and Cohen, J.G. 1980, ApJ, 240, 785
Fusi Pecci, F. 1988, in: Globular Cluster Systems in Galaxies, eds. J.E. Grindlay, A.G.D. Philip, Reidel, Dordrecht, IAU Symp. 126, p.173
Harris, W.E. 1987, in: Stellar Evolution and Dynamics in the Outer Halo of the Galaxy, eds. M. Azzopardi, F. Matteucci, ESO Conf. Workshop Proc. No. 27, Garching, ESO, 683
Harris, W.E. 1991, ARA&A, 29, 543
Harris, W.E., Racine R. 1979, ARA&A, 17, 241
Heasley, J.N, Christian, C.A., Friel, E.D., and Janes, K.A. 1988, AJ, 96,1312
Hodge, P.W. 1979, AJ, 84, 744 (Tab. unpublished)
Hubble, E. 1932, ApJ, 76, 44
Huchra, J.P., Brodie, J.P., Kent, S.M. 1991, ApJ, 370, 495
Iye, M., and Richter, O.-G. 1985, A&A, 144, 471
Johnson, H.L. 1961, ApJ, 133, 109
Makino, J., Akiyama, K., Sugimoto, D. 1990, PASJ 42, 205
Moffat, A.F.J. 1969, A&A, 3, 455
Peterson, R. 1989, in: Dynamics of Dense Stellar Systems, ed. D. Merrit, Cambridge, p. 161
Racine, R. 1991, AJ, 101, 865
Racine, R., and Harris, W.E. 1991, CFH Inf. Bull. No. 24, p.17
Racine, R., and Harris, W.E. 1992, AJ 104, 1068
Rainey, G.W. Jr. 1977, Ph.D. thesis, Univ. of California, Los Angeles
Ratnatunga, K.U., Bahcall, J.N. 1985, ApJS, 59, 63
Reed, L.G., Harris, G.L.H., and Harris, W.E. 1992, AJ, 103, 824
Romeo, G., Bonifazi, A., Fusi Pecci, F., Tosi, M. 1989, MNRAS, 240, 459
Sandage, A.R. 1971, in: Nuclei of Galaxies, ed. J.K. O' Connell, North Holland Publish. Company, Amsterdam, p.222
Sargent, W.L.W., Kowal, C.T., Hartwick, F.D.A., van den Bergh, S. 1977, AJ, 82, 947
Searle, L. 1984, in: Annual Report 1983-1984, Carnegie Institution of Washington, p.32
Sharov, A.S., Lyutyi, V.M. 1986, SvA, 30,371
Sharov, A.S., Lyutyi, V.M. 1989, SvA, 33,235
de Vaucouleurs, G. 1958, ApJ, 128, 465
de Vaucouleurs, G. 1977, AJ, 82, 456
de Vaucouleurs, G. 1978, ApJ, 223, 730
de Vaucouleurs, G. and Buta, R. 1978, AJ, 83, 1383
van den Bergh, S. 1969, ApJS, 19, 145
Vetesnik, M. 1962, Bull. Astr. Inst. Czech, 13, 180
Webbink, R.F. 1985, in: Dynamics of Star Clusters, eds. J. Goodman, P.Hut, Reidel, Dordrecht, p.541
Wirth, A., Smarr, L.L., and Bruno, T.L. 1985, ApJ, 290, 140
Young, P.J. 1976, AJ, 81, 807
Zinn, R.J. 1985, ApJ, 293, 424
Zinn, R.J.5 1986, in: Stellar Populations, eds. C.A. Norman, A. Renzini, and M. Tosi, Cambridge Univ. Press, p. 73

© European Southern Observatory • Provided by the NASA Astrophysics Data System